이학박사학위논문

ASC1의 UFM1결합이 에스트로겐 수용체 알파를 통한 유방암 발달에 미치는 영향에 관한 연구

Studies on the role of ASC1 ufmylation in ERα transactivation and breast cancer development

2014년 2월

서울대학교 대학원

생명과학부

유 희 민

Studies on the role of ASC1 ufmylation in ERα transactivation and breast cancer development

A dissertation submitted in partial
Fulfillment of the requirement for the degree of

DOCTOR OF PHILOSOPHY

To the Faculty of
School of Biological Sciences
at
SEOUL NATIONAL UNIVERSITY
By
Hee Min Yoo

Date Approved:

_____ _____

_____

_____

_____

_____

ASC1의 UFM1결합이 에스트로겐 수용체 알파를 통한 유방암 발달에 미치는 영향에 관한 연구

Studies on the role of ASC1 ufmylation in ERα transactivation and breast cancer development

지도교수 정 진 하

이 논문을 이학박사 학위논문으로 제출함
2013년 11월

서울대학교 대학원
생명과학부
유 희 민

유희민의 이학박사 학위논문을 인준함
2013년 12월

위 원 장 _____ (인)

부위원장 _____ (인)

위 원 _____ (인)

위 원 _____ (인)

위 원 _____ (인)

ABSTRACT

UFM1 (Ubiquitin-fold modifier 1) is a recently identified ubiquitin-like protein (Ubl) based on the similarity of its tertiary structure to ubiquitin (Ub). Similar to Ub and other Ubls, UFM1 is conjugated to cellular proteins via its C-terminal Gly residue by sequential action of the UFM1-activating enzyme UBA5, the UFM1-conjugating enzyme UFC1, and the UFM1 ligase UFL1. UFM1 conjugation is reversible and the release of free UFM1 from target proteins is carried out by two UFM1-specific proteases, UfSP1 and UfSP2. These UfSPs are also responsible for the generation of mature form of UFM1 from its precursors. The UFM1 conjugation and deconjugation systems are well conserved from *C. elegans* to human (but not in yeast or prokaryotes), implicating their critical role in multicellular organisms. However, target proteins for UFM1 modification and the role of this conjugation system remain totally unknown.

By using mass spectrometry, I identified the activating signal cointegrator 1 (ASC1: also called as thyroid hormone receptor interactor 4, TRIP4) as a candidate target protein for UFM1 modification (ufmylation). ASC1 serves as a transcriptional

coactivator of various nuclear receptors, including RARα, steroid receptors, and NF-κB. It forms a complex with other transcriptional coactivators, such as p300 and SRC1, and promotes the transcriptional activity of nuclear receptors.

Under overexpression conditions, ASC1 was poly-ufmylated by the UFM1 system (i.e., UFM1, UBA5, UFC1, and UFL1) in an ATP-dependent manner and this modification could be dramatically stimulated by C20orf116, which had previously been identified as a target substrate for ufmylation. This stimulatory effect required ufmylation of C20orf116, suggesting that C20orf116 serves not only as a target protein but also as a component of the UFM1 system. Since C20orf116 has also been called as UFBP1 based on its ability to bind UFM1, henceforth I recurred C20orf116 to as UFBP1.

ASC1 was indeed found to be conjugated by UFM1 and this modification (ufmylation) was crucial for ERα transactivation and breast tumorigenesis. Without 17β-estradiol, the UFM1-specific protease UfSP2 bound to and deufmylated ASC1. In its presence, however, ERα displaced UfSP2 for binding to and ufmylation of ASC1.

Poly-UFM1 chains conjugated to ASC1 served as a scaffold that recruits p300 and

SRC1 to the promoters of ERα downstream genes, including pS2, CYCLIN D, and c-MYC, for their transcription. ASC1 overexpression or UfSP2 knockdown promoted anchorage-independent cell growth and tumor formation in vivo, whereas overexpression of ufmylation-deficient ASC1 mutant or knockdown of the UFM1-activating enzyme UBA5 prevented them. Furthermore, the expression of UFM1-conjugating machinery, including UBA5, was dramatically up-regulated in ERα-positive human breast tumors. These findings establish the role of ASC1 ufmylation in promotion of ERα transactivation and breast cancer development.

Key word: Ubiquitin-fold modifier 1 (UFM1), UFM1-specific protease (UfSP2), Activating signal cointegrator 1 (ASC1), 17β-estradiol, ERα, Breast cancer

Student Number : 2009-30084

TABLE OF CONTENTS

LIST OF FIGURES

BACKGROUND

1. Ubiquitin-fold modifier 1 (UFM1)

Ubiquitin-fold modifier 1 (UFM1) is the most recently identified ubiquitin-like protein (Komatsu et al., 2004). It shares only 16% identity in the amino acid sequence with ubiquitin, but displays a striking similarity in its tertiary structure to ubiquitin (Figure 1). It has a single Gly at its C-terminus, unlike ubiquitin and most other ubiquitin-like proteins that have a conserved C-terminal di-glycine motif. UFM1 in mouse and human is expressed as a precursor with a C-terminal Ser-Cys di-peptide extension that needs to be processed prior to conjugation to target proteins. The matured UFM1 is specifically activated by an E1-like enzyme, UBA5, transferred to its cognate E2-like enzyme, UFC1, and finally conjugated to target proteins by an E3-like ligase, UFL1 (Komatsu et al., 2004; Mizushima et al., 2007; Tatsumi et al., 2010). The UFM1 system is conserved in metazoa and plants but not in yeast, implicating its important roles in multi-cellular organisms. Intriguingly, the

UFM1 system has recently been shown to play an essential role in the control of erythrocyte differentiation by knocking out *Uba5* gene in mice (Tatsumi et al., 2011).

Like protein modification by ubiquitin and ubiquitin-like proteins, such as SUMO and ISG15, UFM1 modification is a reversible process that is catalyzed by UFM1-specific proteases (UfSPs). Our laboratory has identified two murine UfSPs, named UfSP1 and UfSP2, and determined their X-ray crystallographic structures. UfSP1 and UfSP2, consisting of 217 and 461 amino acids, respectively, are sensitive to inhibition by sulfhydryl-blocking reagents, such as N-ethylmalimide, but have no sequence homology with previously known proteases, suggesting that UfSP1 and UfSP2 are a novel type of thiol proteases (Kang et al., 2007; Ha et al., 2008; Ha et al., 2011). Both proteases are capable of cleaving the C-terminal extension of UFM1 but not that of ubiquitin or other ubiquitin-like proteins. They also can release UFM1 from UFM1-conjugated cellular proteins.

Figure 1. Comparison of the structures of ubiquitin and UFM1.

Ribbon diagram of Ub and UFM1. Global fold of UFM1 is similar to that of ubiquitin (Ub).


Ubiquitin
UFM1
Merge

Figure 2. Summary for the UFM1 modification pathway

The C-terminal amino acids have to be cleaved by C-terminal hydrolases to expose the Val-Gly motif for conjugation. Attachment of UFM1 to lysine residues of target proteins (C20orf116) is catalyzed by E1, E2 and E3 enzymes related to the enzymes in ubiquitination pathway. Ufmylation is reversible, and UFM1 can be removed from target proteins by isopeptidases.

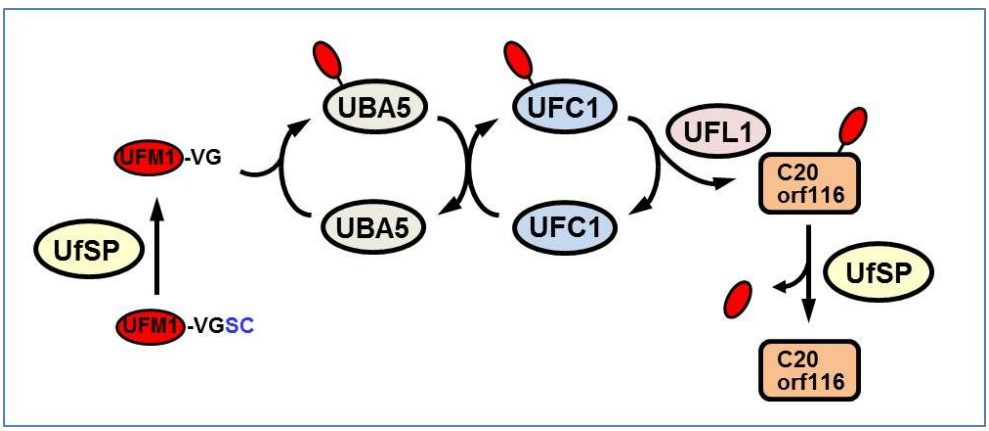
UBA5
UFC1
UFL1
UFM1-VG
C20
orf116
UBA5
UFC1
UfSP
UfSP
UFM1-VGSC
C20
orf116

2. Activating signal cointegrator 1 (ASC1) and other coactivators

ASC1 serves as a transcriptional coactivator of various nuclear receptors, including RXR, steroid receptors, and NF-κB. It forms a complex with other transcriptional coactivators, such as p300 and SRC1, and promotes the transcriptional activity of nuclear receptors (Kim et al., 1999; Lee et al., 1995). ASC1 has an transactivation domain that contains a zinc finger motif, which provides binding sites for basal transcription factors TBP and TFIIA, transcription integrators steroid receptor coactivator 1 (SRC-1) and CBP-p300, and nuclear receptors (Figure 3A). ASC1, a nuclear protein, localizes to the cytoplasm upon serum starvation, but can be translocated to the nucleus when supplemented with ligands or coexpressed with CBP or SRC-1, raising an interesting possibility that ASC-1 may play an important role in establishing distinct coactivator complexes under different cellular conditions (Kim et al., 1999). ASC-1 can also stably form a complex with three additional polypeptides, P200, P100, and P50. These ASC-1 complex appears to play an essential role in AP-1, SRF, and NF-κB transactivation and to mediate the transrepression between nuclear

receptors and either AP-1 or NF-κB in vivo (Jung et al., 2002).

ASC2 is a 250-kDa protein consisting of 2063 amino acids. ASC2 in yeast and in mammalian cells shows a modular structure consisting of an activation domain (AD1), the second Glu/Pro-rich activation domain (AD2), LxxLL-1 motif, which plays an essential role in ligand-dependent interaction with a variety of NRs, LxxLL-2 motif, which is more limited in its NR interaction, a dimerization domain near LxxLL-1, and an inhibitory region at the C terminus rich in Ser, Thr, and Leu residues (Mahajan et al., 2005). Interestingly, the copy-number of ASC2 increases in breast cancer. This high of level of ASC2 in breast cancer cell lines, howver, does not correlate with the level of ERα. In addition, it has been reported that expression of ASC2 mRNA is increased in 11 different breast cancer cell lines with the highest expression in BT-474 cells. The *ASC2* gene is amplified in lung and colon cancers (Lee et al., 1999).

SRCs contain three structural domains. The amino terminal bHLH–PAS [basic helix–loop–helix–Per/aryl hydrocarbon receptor nuclear translocator (ARNT)/Sim] domain is required for protein–protein interaction. The central region contains three

LxxLL motifs, which form amphipathic α-helices and are responsible for interacting with various NRs. The C-terminal region contains two transcriptional activation domains (AD1 and AD2). Signalling pathways that are activated by extracellular stimuli, such as hormones, growth factors and cytokines, induce multiple post-translational modifications of SRCs, including phosphorylation, ubiquitylation, sumoylation, acetylation, and methylation (Xu et al., 2009).

CBP and p300, possessing histone acetyltransfrase (HATs) activity, are highly homologous proteins with a shared domain structure (Goodman and Smolik, 2000). Both p300 (Hanstein et al, 1996) and CBP (Smith et al, 1996) interact with p160 co-regulators as well as with ER at the AF-1 domain in a ligand-dependent manner (Kobayashi et al, 2000). p300 can also directly interact with the AF-2 domain of ER, and can potentiate the synergistic activity resulted from AF-1 and AF-2 interaction (Kobayashi et al., 2000).

3. Estrogen receptor α (ERα) and its signalling pathway

ERα is responsible for many of the effects of estrogens on normal and malignant breast tissues. Lifetime exposure to 17β-estradiol (E_2) constitutes a major risk factor for breast cancer development. ERβ opposes ERα, and inhibits ERα-mediated proliferation (Nilsson et al., 2011; Romancer et al., 2011). Both receptors have a domain structure that is common to other nuclear receptors. The amino-terminal regions contain a transactivation domain (AF1) with ligand-independent function and a co-regulatory domain that is responsible for the recruitment of co-activators and co-repressors. DNA-binding domain (DBD) is required for binding to specific oestrogen response elements (EREs). The C-terminal regions contain the ligand-binding domain (LBD), and have a ligand-dependent transactivation function (Thomas et al., 2011). Figure 3B shows the domain structure of ERα.

Estradiol influences cell proliferation, inflammatory response, and tumour development. Genomic effects of estradiol usually occur via ligand-dependent binding of receptors to target gene promoters (Castoria et al., 2010). The classical mechanism

of ER action involves ligand binding to the ligand-binding domain of the receptor, which induces ligand-specific conformational changes of the protein. Its dissociation from inhibitory heat shock protein complexes allow subsequent phosphorylation and trigger homo- or heterodimerization of ER and binding to specific estrogen response elements (EREs) in target genes (Gougelet et al., 2005; Perissi et al., 2010). The ligand-induced conformational change of the receptor facilitates the recruitment of coregulator complexes for the regulation of chromatin function (Lonard et al., 2006). After the initiation of transcription, post-translational modifications, such as methylation and acetylation, promote the dissociation of the complex, and the simultaneous ubiquitylation of ERs either results in further activation of the receptors or induces their degradation (Robyr et al., 2000).

Approximately 70% of breast cancers express ERα, and this tumorigenic property has been utilized for breast cancer treatment for decades (Shanle et al., 2010). Anti-estrogens, such as selective estrogen receptor modulators (SERMs), which act as competitive blockers of oestrogen–ER binding, and aromatase inhibitors, which target

oestrogen synthesis, have been successfully used for treatment and prevention of breast cancer. However, one-third of the women treated with tamoxifen, one of the most widely used SERMs, for 5 years will have recurrence of the disease within 15 years. Among the mechanisms of de novo or intrinsic endocrine resistance is the lack of ERα expression (Thomas et al., 2011).

Figure 3. Domains structure of ASC1 and ERα

(A) ASC1 contains a zinc finger motif with an arrangement of metal binding residues similar to those of E1A (residues 125 to 237). The red line indicates LxxLL motif, which binds the activation function-2 (AF-2) region of nuclear-receptor. (B) The structural domains are labelled with the amino acid numbers. The N-terminal AF1 domain is involved in transactivation. DNA-binding domain (DBD) is required for binding to specific estrogen response elements (EREs). H region contains several functional domains, including the hinge domain, part of the ligand-dependent activating domain, and the nuclear localization signal. The C-terminal AF2 domains mediates multiple functions, including ligand binding, transactivation, and dimerization.

A

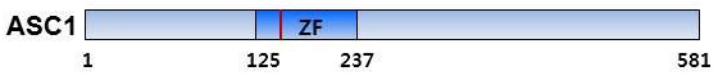

B

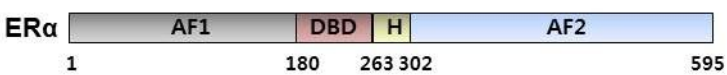

4. Purpose of thesis work

Approximately 70% of human breast cancer is ERα-positive. Therefore, patients with ERα-positive breast cancer have been treated with tamoxifen or aromatase inhibitors, both of which prevent 17β-estradiol-mediated transactivation of ERα. While these treatments are effective, many patients inevitably develop the drug-resistant invasive tumors. Therefore, it is of necessity to identify new targets for development of drugs against ERα-positive breast cancer.

Our laboratory work has been focused on the role of ubiquitin and ubiquitin-like proteins in the control of cancer development (Lee et al., 2006, 2012; Jeon et al., 2012). To this end, I attempted to identify target proteins that are modified by UFM1, which is the most recently identified ubiquitin-like protein (Komatsu et al., 2004) by using double immuno-affinity purification of UFM1-conjugated proteins followed by mass spectrometry. Intriguingly, one of target proteins identified was ASC1, which is known to act as a transcriptional co-activator of hormone-nuclear receptors, including ERα.

In this study, I attempt to find whether 17β-estradiol may induce ASC1 modification by UFM1 and whether this modification is required for ERα transactivation and tumor formation in vivo. Furthermore, I elucidate whether UFM1-conjugating machinery is dramatically up-regulated in ERα-positive tumor tissues, but not in ERα-negative tissues, implicating its ERα-specific oncogenic role. Thus, UFM1-conjugating machinery, including the UFM1-activating enzyme UBA5, would be used as potential targets for development of new therapeutic drugs against ERα-positive breast cancer.

INTRODUCTION

Ubiquitin-fold modifier 1 (UFM1) is the most recently identified ubiquitin-like protein (Komatsu et al., 2004; Schulman and Harper, 2009). Like ubiquitination, protein modification by UFM1 (ufmylation) utilizes a 3-step enzyme system: UBA5 as an UFM1-activating E1 enzyme, UFC1 as an UFM1-conjugating E2 enzyme, and UFL1 as an UFM1 E3 ligase (Mizushima et al., 2007; Tatsumi et al., 2010; Tatsumi et al., 2011). Ufmylation is a reversible process that is catalyzed by UFM1-specific proteases (UfSPs). Our laboratory has recently identified two murine UfSPs, named UfSP1 and UfSP2 (Kang et al., 2007), and determined their X-ray crystallographic structures (Ha et al., 2008; Ha et al., 2011). In human, however, only one functional UfSP2 is expressed (http://www.ncbi.nlm.nih.gov/gene/402682).

The UFM1 system is conserved in metazoan and plants, but not in yeast, implicating its specific roles in multi-cellular organisms. Intriguingly, the UFM1 system has recently been shown to play an essential role in erythrocyte differentiation

by using Uba5 knockout mice (Tatsumi et al., 2011). In addition, UFM1 seems to be involved in ER stress and fatty acid metabolism (Azfer et al., 2006; Gannavaram et al., 2011; Lemaire et al., 2011; Zhang et al., 2012). However, biological functions of the UFM1 system are largely unknown, because so far only one protein C20orf116 has been identified as a target (Mizushima et al., 2007; Tatsumi et al., 2010; Tatsumi et al., 2011). Neither the functional significance of C20orf116 ufmylation is known.

Estrogen receptor-α (ERα), a member of the nuclear receptor superfamily, is prominent in breast cancer (Green and Carroll, 2007; Liang and Shang, 2013; Osborne and Schiff, 2011). Upon binding of 17β-estradiol (henceforth referred to as E_2), ERα undergoes a major conformational change to form a dimeric complex, translocates to the nucleus, recruits transcriptional co-activators, such as SRC1 and p300, and binds to ER-responsive elements (ERE), located in the promoters of target genes, including pS2, cyclin D, and c-Myc, for their transcriptional activation (Klinge, 2001; Nilsson et al., 2001). Thus, ERα is known as a growth factor that is essential for proliferation of a large subset of breast tumor cells.

Activating signal co-integrator 1 (ASC1), originally identified as thyroid hormone receptor interactor 4 (TRIP4), is a transcriptional co-activator of ERα as well as of other nuclear receptors (e.g., AR and TR) (Kim et al., 1999; Lee et al., 1995; Xu et al., 2009). ASC1 has a zinc finger domain, which serves as a binding site for nuclear receptors, transcriptional co-activators (e.g., p300 and SRC1), and basic transcriptional machinery (e.g., TBP and TFIIA). Thus, ASC1 appears to play a critical role as a platform that recruits the necessary components for nuclear receptor-mediated transcription. However, it is mechanically unclear how the zinc finger domain, a short region within ASC1 (amino acids 125-237), can simultaneously bind such a group of the proteins.

Post-translational protein modifications by ubiquitin and ubiquitin-like proteins (e.g., SUMO and ISG15) play important roles in the control of numerous cellular processes (Hermanson et al., 2002; Hoeller et al., 2006; Jeon et al., 2010). In particular, Lys63-linked poly-ubiquitin chains serve as a scaffold for formation of protein complexes that propagate various signals, such as for apoptosis and immune

responses (Kulathu and Komander, 2012). Transcriptional co-activators and co-repressors are known to undergo diverse post-translational modifications, including phosphorylation, methylation, acetylation, sumoylation, and ubiquitination, for the control of nuclear receptor function (Hassig and Schreiber, 1997; Lee et al., 2005; Lonard and O'Malley B, 2007; Schmidt and Muller, 2003; Shao et al., 2004; Wu et al., 2006). Thus, it appears possible that ASC1 adopts similar types of modification, such as by ubiquitin or ubiquitin-like proteins, for facilitating the recruitment of required proteins and conveying the signals for transactivation of nuclear receptors.

In this study, I demonstrated that ASC1 is a novel target for ufmylation and C20orf116 is an essential component for ASC1 ufmylation as well as a substrate. Of the six Lys residues in UFM1, only Lys69 was used in the formation of poly-UFM1 chains via isopeptide bonds. In addition, I identified the Lys324, Lys325, Lys334, and Lys367 residues in ASC1 as the UFM1 acceptor sites. Remarkably, ufmylation of endogenous ASC1 occurred only when cells were treated with E_2. Without E_2, UfSP2, a UFM1-specific protease, bound to the zinc-finger domain of ASC1 and prevented

ufmylation. In its presence, however, ERα displaced UfSP2 for binding to the domain and allowed ASC1 ufmylation. Poly-UFM1 chains formed on ASC1 served as a scaffold for recruiting p300 and SRC1 to the promoters of ERα target genes. Furthermore, ASC1 overexpression or UfSP2 knockdown promoted the transcriptional activation of ERα target genes, anchorage-independent colony formation, and tumor formation in vivo. In contrast, overexpression of ufmylation-deficient ASC1 mutant or UBA5 knockdown abrogated them. Remarkably, UFM1-conjugating machinery (i.e., UBA5, UFC1, UFL1, and C20orf116) were markedly up-regulated in ERα-positive breast tumors, but not in ERα-negative tumors. Taken together, these results indicate that E_2-mediated ASC1 ufmylation plays a crucial role in breast cancer development by promoting ERα transactivation.

MATERIALS AND METHODS

1. Plasmids and antibodies

The cDNA for ASC1 (KUGI, Korea) was cloned into pcDNA4-HisMax, pCMV2-Flag, and pcDNA3.1-Myc. It was also cloned into pQE-30 and pGEX-4T-1 for bacterial expression. shRNAs were purchased from Open Biosystems. Target sequences used for shRNAs were: TGATGAGGAAGAAGGTCCT for ASC1; AACAGAAACTTTAACACGT for UBA5; AATAACTTGCAGGTCTTCAGC for UfSP2; TGATGTAGTTGATGAACTC for UFBP1 (all from 5' to 3'). Antibodies against C20orf116 (G-17), UFM1 (I-16), UfSP2 (C-7), ERα (H-184), SRC1 (C-20), p300 (C-20), and c-Myc (9E10) were purchased from Santacruz. Anti-ASC1, anti-UFL1 (Bethyl Laboratories), anti-UBA5, anti-UFC1 (Abcam), anti-Flag M2 (Sigma-Aldrich), anti-Xpress (Invitrogen), and anti-His (BD Biosciences) antibodies were also used.

2. Cell culture and transfection

HEK293T and MCF7 cells were grown at 37°C in DMEM (Hyclone) supplemented with 100 units/ml of penicillin, 1 μg/ml of streptomycin, and 10% FBS (Hyclone). In place of DMEM, RPMI1640 (Hyclone) was used for culturing BT-474, MDA-MB-231, and PC-3 cells and MEM (Hyclone) was for LNCaP cells. MCF10A cells were cultured as described (Jeon et al., 2012). Plasmids were transfected to cells using Metafectene reagent (Biontex), jetPEI™ DNA Transfection Reagent (Polyplus-transfection), Lipofectamine with PLUS reagent (Invitrogen), or Neon™ Transfection System (Invitrogen).

3. Assays for UFM1 modification

HisMax-ASC1, Flag-UFM1, and Myc-tagged UBA5, UFC1, UFL1, and UFBP1 were overexpressed in HEK293T cells. After culturing for 36 h, cells were lysed by boiling for 20 min in 150 mM Tris-HCl (pH 8), 5% SDS, and 30% glycerol. Cell lysates were diluted 20 fold with buffer-A consisting of 50 mM Tris-HCl (pH 8.0),

150 mM NaCl, 10 mM imidazole, 1% Triton X-100 or 0.5% NP-40, 1X protease inhibitor cocktail, and 2 mM NEM. After incubating them with NTA resins for 3 h at 4°C, precipitates were washed with buffer-A containing 20 mM imidazole, and boiled in SDS-sampling buffer. Supernatants were subjected to SDS-PAGE followed by immunoblot analysis.

4. Immunoprecipitation

Cells were lysed in 50 mM Tris-HCl (pH 8) containing 50 mM Tris-HCl (pH 8.0), 150 mM NaCl, 1% Triton X-100 or 0.5% NP-40, 1X protease inhibitor cocktail (Roche), and 2 mM NEM. Cell lysates were incubated with appropriate antibodies for 2 h at 4°C and then with 30 μl of 50% slurry of protein A-Sepharose (Sigma) for 1 h. The resins were collected by centrifugation, and boiled in SDS-sampling buffer. The samples were then subjected to immunoblot analysis.

5. Purification of recombinant proteins

For protein purification, E. coli BL21 (DE3) cells transformed with pQE30-ASC1, pMAL-UFL1, and pGEX6P-UFBP1 were grown in Luria broth. Cell extracts were subjected to column chromatography using Ni^{2+}-NTA agarose (Qiagen), amylose-conjugated Sepharose (New England BioLabs), and GSH-Sepharose 4B (GE Healthcare) for purification of His-ASC1, MBP-UFL1, and GST-UFBP1, respectively. Proteins bound to the columns were eluted as recommended by the manufacturers.

6. RT-PCR and real-time quantitative PCR

Total RNAs were isolated from cells by using TRIzol (Invitrogen). RT-PCR was performed using SuperScript III (Invitrogen), according to the manufacturer's instructions. The resulting mRNAs were quantified by qPCR using the ABI Prism 7700 sequence detection system (Applied Biosystems). Primers used in qPCR were: GGTCGCCTTGGAGCAGA and GGGCGAAGATCACCTTGTT for pS2; GCTGCTCCTGGTGAACAAGC and AAGTGTTCAATGAAATCGTGCG for cyclin D1; TCCACACATCAGCACAACTACG and

CACTGTCCAACTTGACCCTCTTG for c-Myc (all from 5' to 3').

7. Luciferase assays

MCF7 cells transfected with pcDNA-β-Gal and ERE-Luc were incubated for 24 h. After E_2 (Sigma) treatment, cells were incubated for 24 h, harvested, and assayed for luciferase. The enzyme activity was measured in a luminometer and normalized by β-galactosidase expression with a luciferase system (Promega).

8. Chromatin immunoprecipitation (ChIP) assay

MCF7 cells that had been treated with E_2 for 1 h were subjected to ChIP analysis. ASC1-DNA complexes were subjected to immunoprecipitation with anti-ASC1 antibody. DNAs were extracted from the precipitates, and aliquots of them were subjected to qPCR analysis. Primers used for the pS2 promoter were: 5′ -primer, CGTGAGCCACTGTTGTCAGG; 3′ -primer, TGGTGAGGTCATCTTGGCTG.

9. MTT assay

MCF-7 cells stably expressing shRNAs were plated at a density of 2 x 10^4 cells per well in 24-well plates, and grown in the presence or absence of 10 nM E_2. Cell proliferation was determined by incubation with 4,5-dimethyl-2-yl 2,5-diphenyl thiazoyl blue tetrazolium bromide (MTT, AMRESCO) for 4 h. After incubation, culture medium was replaced by 100 μl of DMSO. Absorbance at 540 nm was then measured by using a Biokinetics plate reader (Bio-Tek Instruments).

10. Immunocytochemistry

MCF7 cells were grown on coverslips. After transfection, they were fixed by incubation with 3.7% paraformaldehyde in PBS for 10 min. Cells were washed three times with PBS containing 0.1% Triton X-100, and permeabilized with 0.5% Triton X-100 in PBS for 5 min. After blocking with 3% BSA in PBS for 30 min, cells were incubated overnight at 4'C with appropriate antibodies. After washing with PBS containing 0.1% Triton X-100, cells were incubated for 1 h with FITC- or TRITC-

conjugated secondary antibody in PBS containing 3% BSA. Cells were then observed using a confocal laser scanning microscope (Carl Zeiss-LSM700).

11. Immunohistochemistry

Tumor tissues were embedded in OCT. Cryosections (10 μm) were permeabilized and fixed with methanol. Sections were then incubated with 3% H_2O_2 in PBS for 10 min to quench endogenous peroxidase activity. After treatment with a blocking solution (5% horse serum, 3% bovine serum albumin, and 0.1% Triton X-100 in PBS), they were incubated with primary antibodies in blocking solution overnight at 4°C. Sections were washed and incubated with horseradish peroxidase-conjugated secondary antibodies for 2 h at room temperature. Signals were detected using 3,3'-diaminobenzidine as a substrate. They were then counterstained with hematoxylin.

12. Colony formation and tumorigenesis assay

For colony formation assay, cells (2×10^4) were resuspended in 0.35% agar in

DMEM supplemented with 10% FBS. They were then overlaid on 0.7% agar in the same medium in 6-well plates. The plates were incubated at 37°C in 5% CO_2 for 5 weeks. Colonies were stained with 0.005% crystal violet and counted. For in vivo tumorigenesis assay, MCF7 cells (5×10^6) stably expressing shRNAs and those overexpressing ASC1 or its 4KR mutant were subcutaneously injected into the upper thigh of one leg of 6-week-old BALB/c nude mice (Orient Bio Inc.). On the third day after injection, mice began receiving 1 μg/ml of E_2. They were monitored regularly for tumor growth. When tumors grow to appreciable sizes, mice were killed and tumors were dissected out. Tumor volumes were calculated as (a x a x b)/2, in which 'a' is the smallest diameter and 'b' the largest.

RESULTS

1. Identification of ASC1 as a target for ufmylation and its interaction with C20orf116

To identify targets for ufmylation, I performed double immuno-affinity purification by stable expression of Flag-His-UFM1 in NIH3T3 cells (Figure 4A). Ufmylated proteins were first enriched by pull-down from the cell lysates with NTA resins. Proteins bound to the resins were eluted, and ufmylated proteins in the eluates were again enriched by pull-down with anti-Flag antibody-conjugated resins. Precipitated proteins were subjected to SDS-PAGE (Figure 4B) and mass spectrometry. Figure 4C shows the identified candidate proteins for ufmylation. Of these, I chose ASC1 for further investigation to determine the role of its ufmylation in nuclear receptor-mediated transcription.

Figure 4. Identification of ASC1 as a target for ufmylation

(A) Strategy for identification of targets for ufmylation. (B) Identification of ASC1 as a target for ufmylation. Proteins eluted from the resins were subjected to SDS-PAGE followed by immunoblot or silver-stained. (C) List of the candidate target proteins identified by mass spectrometry.

A

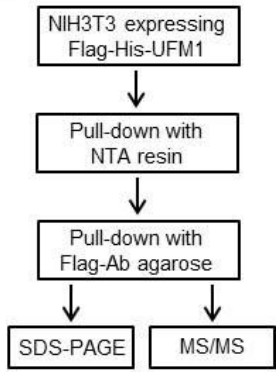

B

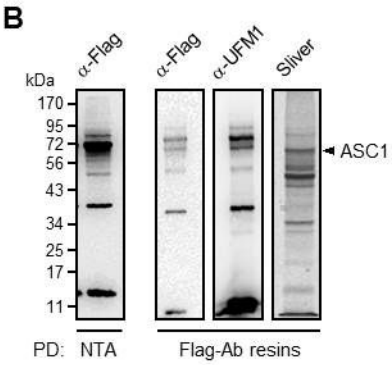

C

Proteins	Full names
ARCN1	Archain 1
DEAD2	DEAD-box RNA helicase
DDX1	DEAD (Asp-Glu-Ala-Asp) box polypeptide 1
DNAJC1	DnaJ (Hsp40) homolog, subfamily C, member 10
ASC1	**Activating signal co-integrator 1**
SMAD5	MAD homolog 5
TRAP1	TNF receptor-associated protein 1
ZBTB12	Zinc finger and BTB domain containing 12
KE4	Zinc transporter SLC39A7
TRIM16	Tripartite motif containing 16
ORFR561	Olfactory receptor 561
LZAP	Putative tumor suppressor, inhibiting NFκB

C20orf116 has been identified as a target for ufmylation (Tatsumi et al., 2010). Notably, C20orf116 has been shown to interact with LZAP (Kwon et al., 2010), which I identified as one of the candidate proteins for ufmylation (Figure 4C), suggesting that C20orf116 might also interact with other targets. Immunoprecipitation analysis showed that C20orf116 is capable of interacting with ASC1 (Figure 5A) and human KE4 (HKE4) (Figure 5B), which were identified as targets for ufmylation (Figure 4C). In addition, purified ASC1 interacted with GST-C20orf116, but not with GST (Figure 6), indicating that C20orf116 directly binds to ASC1. Moreover, the endogenous UFL1, C20orf116, and ASC1 proteins interact with each other, indicating that the three proteins can form a ternary complex (Figure 7). These results suggest that C20orf116 has an unknown function related to protein ufmylation in addition to being a substrate protein.

Figure 5. C20orf116 interacts with ASC1 and HKE4

(A) C20orf116-Myc (C20-Myc) was expressed in HEK293T cells with Flag-ASC1. Cell lysates were subjected to immunoprecipitation with anti-Flag or anti-Myc antibody followed by immunoblot with anti-Myc and anti-Flag antibodies. They were also directly probed with the same antibodies. (B) Experiments were performed as in (A), except the use of C20orf116-Flag and Myc-HKE4 in place of C20orf116-Myc and Flag-ASC1, respectively.

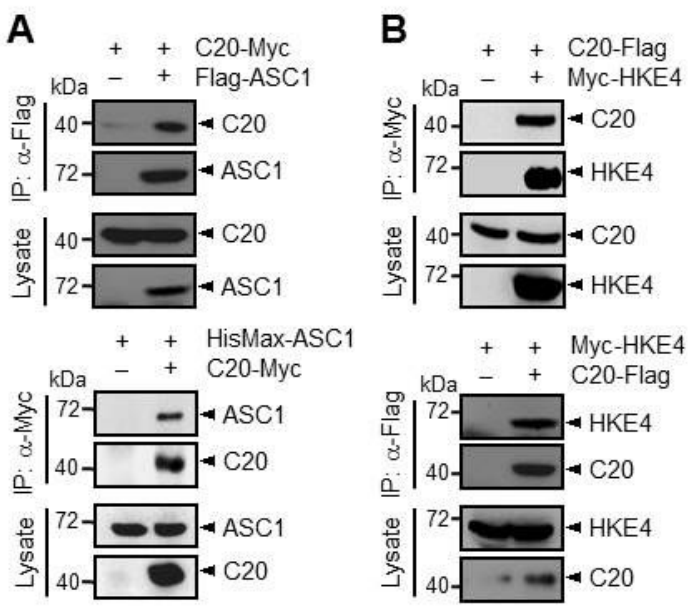
A
+ + C20-Myc
– + Flag-ASC1
kDa
IP: α-Flag
40
72
C20
ASC1
Lysate
40
72
C20
ASC1
+ + HisMax-ASC1
– + C20-Myc
kDa
IP: α-Myc
72
40
ASC1
C20
Lysate
72
40
ASC1
C20
B
+ + C20-Flag
– + Myc-HKE4
kDa
IP: α-Myc
40
72
C20
HKE4
Lysate
40
72
C20
HKE4
+ + Myc-HKE4
– + C20-Flag
kDa
IP: α-Flag
72
40
HKE4
C20
Lysate
72
40
HKE4
C20

Figure 6. C20orf116 directly binds to ASC1

Purified His-ASC1 was incubated with GST or GST-C20orf116 followed by pull-down (PD) with glutathione-Sepharose (GSH-resin).

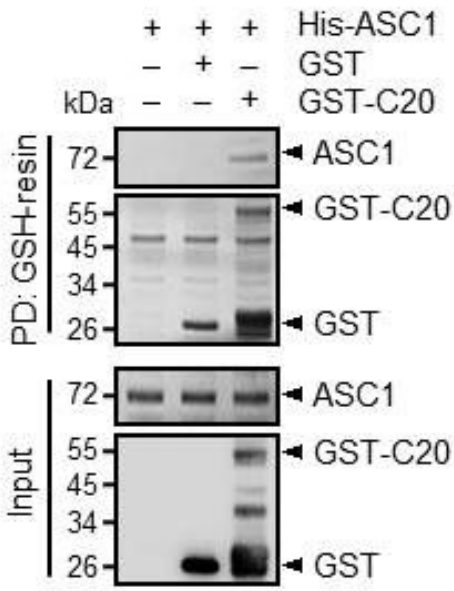
+ + + His-ASC1
– + – GST
kDa – – + GST-C20
PD: GSH-resin
72
55
45
34
26
ASC1
GST-C20
GST
Input
72
55
45
34
26
ASC1
GST-C20
GST

Figure 7. ASC1 forms a ternary complex with UFL1 and C20orf116

Cell lysates were subject to immunoprecipitation with IgG or anti-ASC1 or anti-C20orf116 antibody followed by immunoblot analysis.

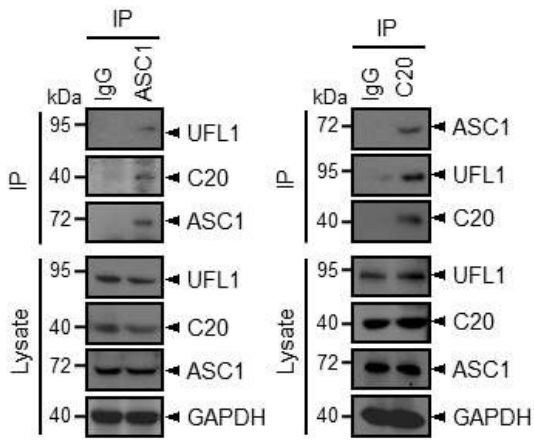
IP
IgG
ASC1
kDa
IP
95
UFL1
40
C20
72
ASC1
Lysate
95
UFL1
40
C20
72
ASC1
40
GAPDH
IP
IgG
C20
kDa
IP
72
ASC1
95
UFL1
40
C20
Lysate
95
UFL1
40
C20
72
ASC1
40
GAPDH

To locate the regions for binding among ASC1, C20orf116, and UFL1, their deletion constructs were generated and subjected to pull-down analysis. C20orf116 bound to the region of amino acids 200-300 in ASC1 (Figure 8A), and ASC1 bound to the region (118-216) containing the coiled-coil domain in C20orf116, which is important for protein-protein interaction (Figure 8B). ASC1 bound to the region of amino acids 200-400 in UFL1 (Figure 9A), and UFL1 bound to the region of amino acids 300-400 in ASC1 (Figure 9B). Finally, UFL1 bound to the C-terminal region (216-314) of C20orf116 (Figure 10). In addition, C20orf116 is known to bind the N-terminal region (1-200) of UFL1 (Tatsumi et al., 2010). These results indicate that each of ASC1, UFL1, and C20orf116 has two distinct binding sites for the other two proteins, which would allow the formation a ternary complex.

Figure 8. Identification of the binding regions within ACS1 and C20orf116

(A) Deletions of ASC1 were generated, tagged with HisMax to their N-termini, and expressed in HEK293T cells with Flag-C20orf116. Cell lysates were subjected to pull-down with anti-Flag M2 antibody-conjugated resins followed by immunoblot with anti-Flag or anti-Xpress antibody. (B) Deletions of C20orf116 were generated, tagged with Flag to their C-termini, and expressed with HisMax-ASC1. Cell lysates were subjected to pull-down with NTA resins followed by immunoblot with anti-Xpress or anti-Flag antibody.

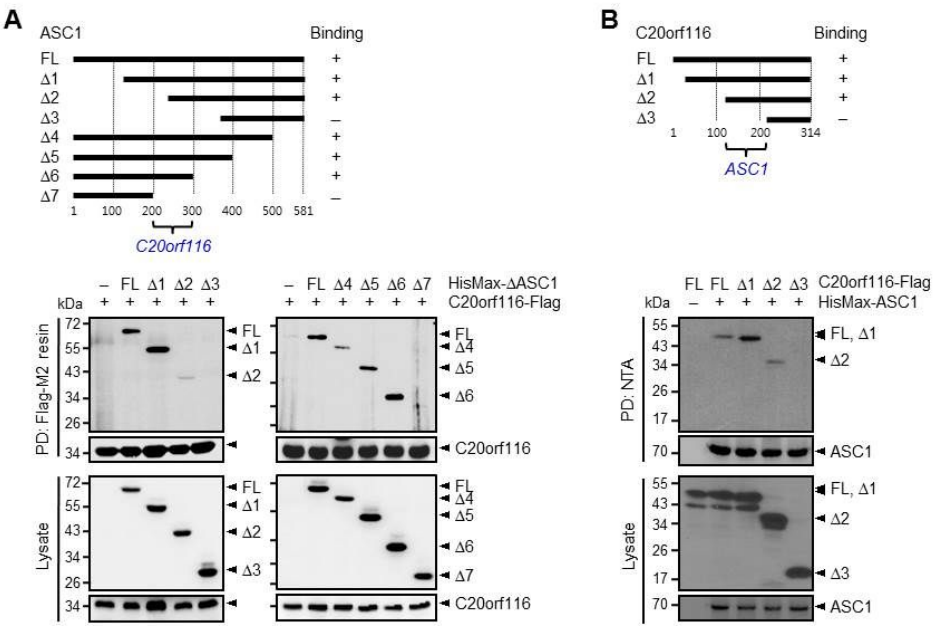
A
ASC1
Binding
FL
Δ1
Δ2
Δ3
Δ4
Δ5
Δ6
Δ7
1 100 200 300 400 500 581
C20orf116
B
C20orf116
Binding
FL
Δ1
Δ2
Δ3
1 100 200 314
ASC1
kDa
HisMax-ΔASC1
C20orf116-Flag
PD: Flag-M2 resin
Lysate
C20orf116
C20orf116-Flag
HisMax-ASC1
PD: NTA
FL, Δ1
ASC1

Figure 9. Identification of the binding regions within ACS1 and UFL1

(A) Deletions of UFL1 were generated, tagged with Myc to their N-termini, and expressed with HisMax-ASC1. Cell lysates were subjected to pull-down with NTA resins followed by immunoblot with anti-Myc or anti-Xpress antibody. (B) Deletions of ASC1 were generated, tagged with HisMax to their N-termini, and expressed with Myc-UFL1. Cell lysates were subjected to pull-down with NTA resins followed by immunoblot with anti-Myc or anti-Xpress antibody.

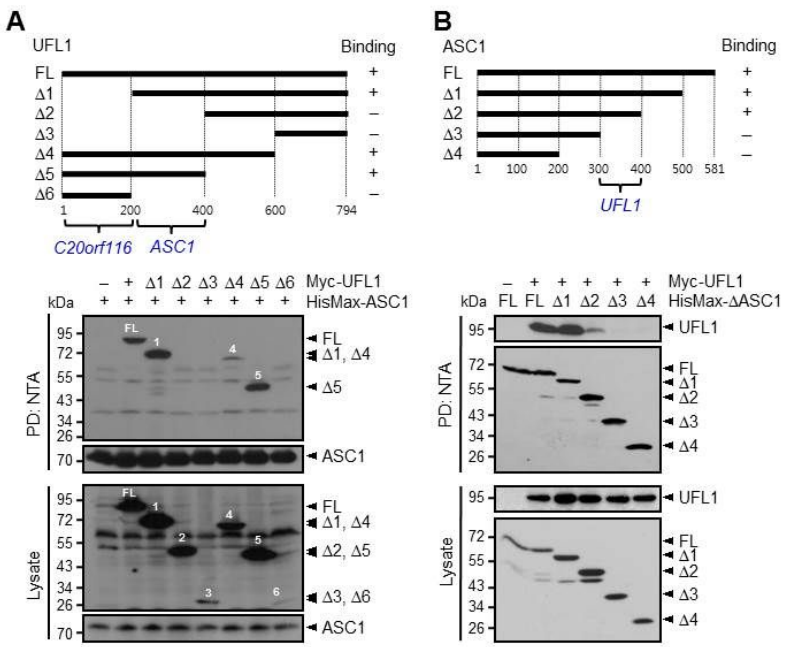
A
UFL1
Binding
FL
Δ1
Δ2
Δ3
Δ4
Δ5
Δ6
1
200
400
600
794
C20orf116
ASC1
– + Δ1 Δ2 Δ3 Δ4 Δ5 Δ6 Myc-UFL1
kDa + + + + + + + + + HisMax-ASC1
PD: NTA
Lysate
95
72
55
43
34
26
70
FL
Δ1, Δ4
Δ5
ASC1
Δ2, Δ5
Δ3, Δ6
B
ASC1
Binding
1
100
200
300
400
500
581
UFL1
– + + + + + Myc-UFL1
kDa FL FL Δ1 Δ2 Δ3 Δ4 HisMax-ΔASC1
UFL1
Δ1
Δ2
Δ3
Δ4

Figure 10. Identification of the binding regions within C20orf116 and UFL1

Deletions of C20orf116 were generated, tagged with Flag to their C-termini, and expressed with HisMax-UFL1. Cell lysates were subjected to pull-down with NTA resins followed by immunoblot with anti-Flag or anti-Xpress antibody.

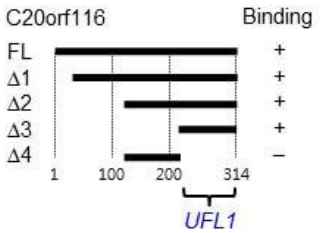
C20orf116
Binding
FL
Δ1
Δ2
Δ3
Δ4
+
+
+
+
–
1
100
200
314
UFL1

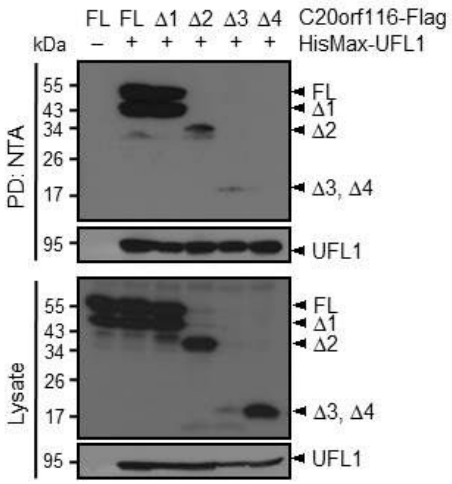
FL FL Δ1 Δ2 Δ3 Δ4 C20orf116-Flag
kDa – + + + + + HisMax-UFL1
PD: NTA
55
43
34
26
17
95
FL
Δ1
Δ2
Δ3, Δ4
UFL1
Lysate
55
43
34
26
17
95
FL
Δ1
Δ2
Δ3, Δ4
UFL1

2. Requirement of C20orf116 for ASC1 ufmylation

To determine whether ASC1 can indeed be modified by UFM1, ASC1 was overexpressed in HEK293T cells with UBA5 (E1), UFC1 (E2), UFL1 (E3), UFM1, and C20orf116 or with all but omitting each of them. The level of ufmylated ASC1 was much higher in the presence of C20orf116 than in its absence (Figure 11). Similar results were obtained when HKE4 was used as a substrate (Figure 12), indicating that C20orf116 acts as a cofactor for ufmylation of target proteins. Since C20orf116 has also been called as UFBP1 based on its ability to bind UFM1 (Lemaire et al., 2011), henceforth I recurred C20orf116 to as UFBP1. Notably, ASC1 could be ufmylated without overexpression of UFBP1 or UBA5, but not without UFM1, UFC1, or UFL1. However, expression of shRNAs specific to UFBP1 (referred to as shUFBP1) and UBA5 (shUBA5), but not a nonspecific shRNA (shNS), abrogated ASC1 ufmylation (Figures 13). These results indicate that ASC1 ufmylation seen without ectopically expressed UFBP1 and UBA5 (Figure 11) is mediated by their endogenous proteins. Since overexpression of UBA5 was not necessary for ufmylation of ASC1 and HKE4,

henceforth I used UFC1, UFL1, and UFBP1 as UFM1-conjugating system.

Figure 11. UFBP1 promotes ASC1 ufmylation

Myc-tagged UBA5, UFC1, UFL1, and UFBP1 were expressed in HEK293T cells with Flag-UFM1 and HisMax-ASC1 as indicated. Cell lysates were subjected to pull-down with NTA resins followed by immunoblot with anti-Flag or anti-Xpress antibody.

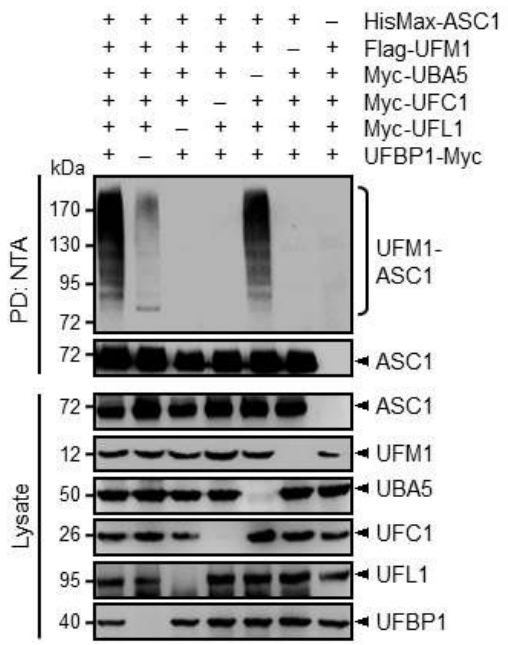
+ + + + + + – HisMax-ASC1
+ + + + + – + Flag-UFM1
+ + + + – + + Myc-UBA5
+ + + – + + + Myc-UFC1
+ + – + + + + Myc-UFL1
+ – + + + + + UFBP1-Myc
kDa
PD: NTA
170
130
95
72
72
UFM1-
ASC1
ASC1
Lysate
72
12
50
26
95
40
ASC1
UFM1
UBA5
UFC1
UFL1
UFBP1

Figure 12. Requirement of UFBP1 (C20orf116) for HKE4 ufmylation

Myc-tagged UBA5, UFC1, UFL1, and UFBP1 were expressed in HEK293T cells with Flag-UFM1 and HisMax-ASC1 as indicated. Cell lysates were subjected to pull-down with NTA resins followed by immunoblot with anti-Flag antibody.

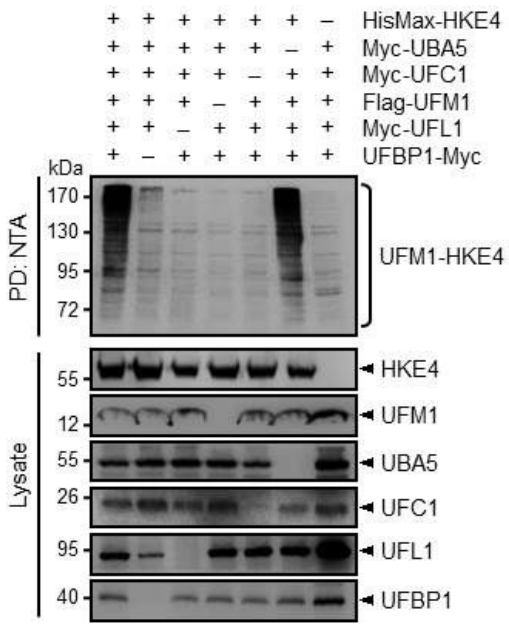
+ + + + + + – HisMax-HKE4
+ + + + + – + Myc-UBA5
+ + + + – + + Myc-UFC1
+ + + – + + + Flag-UFM1
+ + – + + + + Myc-UFL1
+ – + + + + + UFBP1-Myc
kDa
170
130
95
72
PD: NTA
UFM1-HKE4
Lysate
55
HKE4
12
UFM1
55
UBA5
26
UFC1
95
UFL1
40
UFBP1

Figure 13. Knockdown of UFBP1 or UBA5 prevents ASC1 ufmylation

HisMax-ASC1 and UFM1-conjugating system were expressed with shUFBP1 (A) or shUBA5 (B).

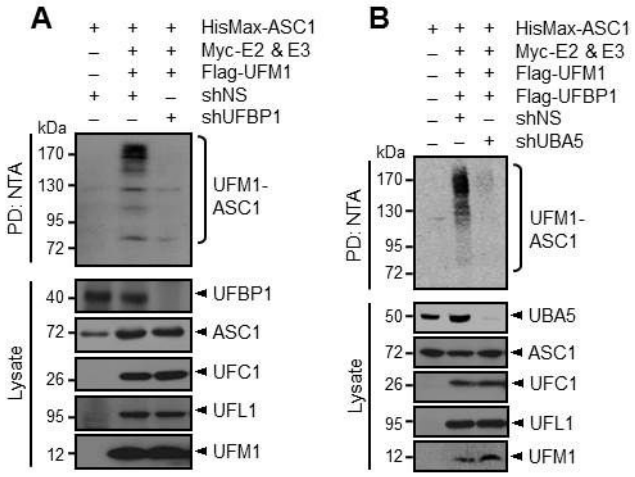
A
+ + + HisMax-ASC1
– + + Myc-E2 & E3
– + + Flag-UFM1
+ + – shNS
– – + shUFBP1
kDa
PD: NTA
170
130
95
72
UFM1-
ASC1
Lysate
40
72
26
95
12
UFBP1
ASC1
UFC1
UFL1
UFM1
B
+ + + HisMax-ASC1
– + + Myc-E2 & E3
– + + Flag-UFM1
– + + Flag-UFBP1
– + – shNS
– – + shUBA5
kDa
PD: NTA
170
130
95
72
UFM1-
ASC1
Lysate
50
72
26
95
12
UBA5
ASC1
UFC1
UFL1
UFM1

Previously, it has been shown that the ufmylation site in UFBP1 is Lys267 and the replacement of the Lys residue by Arg prevents UFBP1 ufmylation (Tatsumi et al., 2010). Remarkably, the K-to-R mutation of UFBP1 abolished ASC1 ufmylation (Figure 14). Moreover, the low level of ASC1 ufmylation seen without UFBP1 was blocked by overexpression of the K267R mutant, suggesting that the mutant acts dominant negatively against endogenous UFBP1. These results indicate that ufmylation of UFBP1 itself is required for ASC1 ufmylation. In an attempt to determine the role of UFBP1 ufmylation, I compared the ability of the K267R mutant to interact with ASC1 and UFL1 to that of wild-type UFBP1. The KR mutation showed little or no effect on the interaction between UFBP1 and ASC1 (Figure 15A). On the other hand, wild-type UFBP1 interacted much better with UFL1 than its K267R mutant (Figure 15B). Furthermore, knockdown of UBA5 by shUBA5 markedly reduced the binding between endogenous UFL1 and UFBP1 proteins (Figure 15C). These results suggest that ufmylation of UFBP1 is required for its tight binding to UFL1 and in turn for promotion of the E3 ligase activity.

Figure 14. The K267R mutation of UFBP1 prevents ASC1 ufmylation

Myc-tagged UFBP1 (Wt) or its K267R mutant (KR) was expressed with HisMax-ASC1 and UFM1-conjugating system.

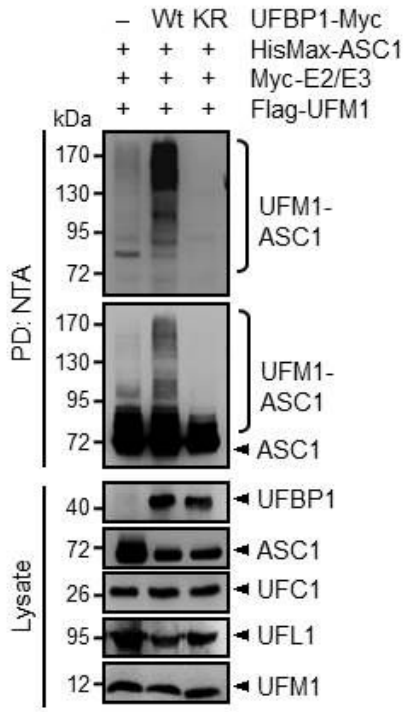
– Wt KR UFBP1-Myc
+ + + HisMax-ASC1
+ + + Myc-E2/E3
+ + + Flag-UFM1
kDa
PD: NTA
170
130
95
72
UFM1-
ASC1
170
130
95
72
UFM1-
ASC1
ASC1
Lysate
40
UFBP1
72
ASC1
26
UFC1
95
UFL1
12
UFM1

Figure 15. The K267R mutation blocks the binding of UFBP1 to UFL1, but not to ASC1

Flag-tagged UFBP1 or its K267R mutant was expressed with Myc-tagged ASC1 (A) or UFL1 (B). (C) UBA5 knockdown inhibits the binding of UFBP1 to UFL1. Cells were transfected with shNS or shUBA5 followed by immunoprecipitation with anti-UFBP1 antibody.

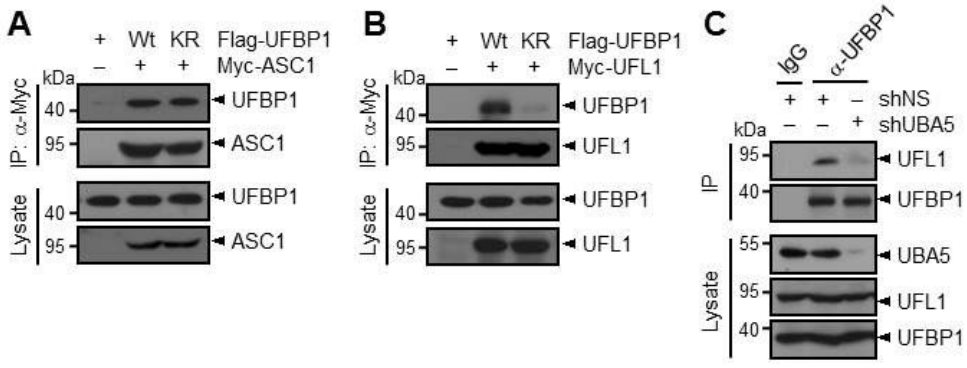
A
+ Wt KR Flag-UFBP1
– + + Myc-ASC1
kDa
IP: α-Myc
40
95
UFBP1
ASC1
Lysate
40
95
UFBP1
ASC1
B
+ Wt KR Flag-UFBP1
– + + Myc-UFL1
kDa
IP: α-Myc
40
95
UFBP1
UFL1
Lysate
40
95
UFBP1
UFL1
C
IgG
α-UFBP1
+ + – shNS
– – + shUBA5
kDa
IP
95
40
UFL1
UFBP1
Lysate
55
95
40
UBA5
UFL1
UFBP1

3. Formation of poly-UFM1 chain via K69-linked isopeptide bonds

UFM1 has six Lys residues. To identify the Lys residues that are involved in the formation of poly-UFM1 chains on ASC1, each of them were replaced by Arg. The mutation of the 69th Lys, but none of the others, prevented the chain formation (Figure 16A), indicating that Lys69 serves as the acceptor site in UFM1. To confirm this finding, all Lys residues, except one each of them, were substituted with Arg. None of the UFM1 variants, except the one having Lys69, was capable of forming poly-UFM1 chains on ASC1 (Figure 16B). Neither the Lys-less UFM1 could form the chains. These results indicate that UFM1 forms poly-UFM1 chains via Lys69-linked isopeptide bonds.

Figure 16. Poly-UFM1 chains are formed via K69-linked isopeptide bonds

(A) Each of 6 Lys residues in ASC1 was replaced by Arg. (B) All Lys residues, except one each of them, were replaced by Arg. K0 denotes Lys-less UFM1.

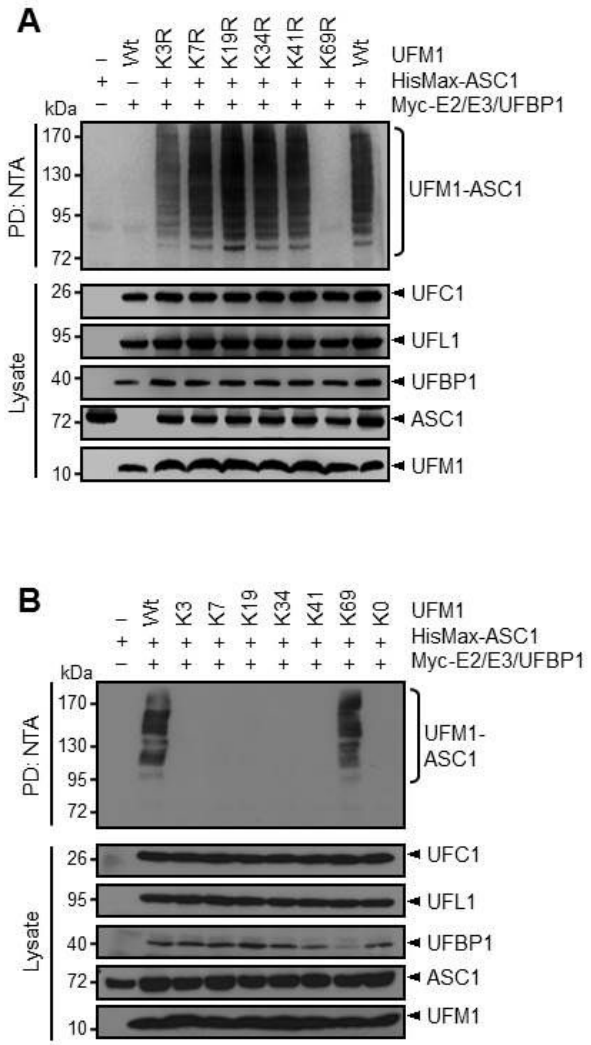
A
UFM1
HisMax-ASC1
Myc-E2/E3/UFBP1
kDa
PD: NTA
UFM1-ASC1
Lysate
UFC1
UFL1
UFBP1
ASC1
UFM1
B
UFM1
HisMax-ASC1
Myc-E2/E3/UFBP1
kDa
PD: NTA
UFM1-
ASC1
Lysate
UFC1
UFL1
UFBP1
ASC1
UFM1

The matured form of UFM1 has a single Gly residue at its C-terminus, unlike ubiquitin and many other ubiquitin-like proteins, such as SUMO and NEDD8, which have di-Gly. Replacement of the Gly residue by Ala prevented the formation of poly-UFM1 chains on ASC1 (Figure 17A), indicating its participation in isopeptide linkage formation. Figure 17B shows the location of Lys69 and Gly83 in the 3D structure of UFM1 (PBD ID: 1WXS) (Sasakawa et al., 2006). Notably, UBA5 has been shown to also act as a SUMO2-activating E1 enzyme under both in vivo and in vitro conditions (Zheng et al., 2008). Therefore, I examined whether UFM1-conjugating system with UBA5 might be able to form polymeric chains of SUMO2 or other ubiquitin-like proteins on ASC1. However, it allowed only poly-UFM1 chain formation (Figure 17C), indicating the system is specific to UFM1.

Figure 17. The C-terminal Gly of UFM1 is required for ASC1 ufmylation

(A) The C-terminal Gly was replaced by Ala in UFM1 having a Lys residue only at the 69th position. (B) The 3D structure of UFM1 (PBD ID: 1WSX). (C) UFM1-specific Modification of ASC1. HisMax-ASC1 was expressed in HEK293T cells with UBA5, UFC1, UFL1, and UFBP1 in the presence of Flag-tagged UFM1, ubiquitin, ISG15, SUMO1, SUMO2, or Nedd8. Cell lysates were subjected to pull-down with NTA resins followed by immunoblot with anti-Flag antibody.

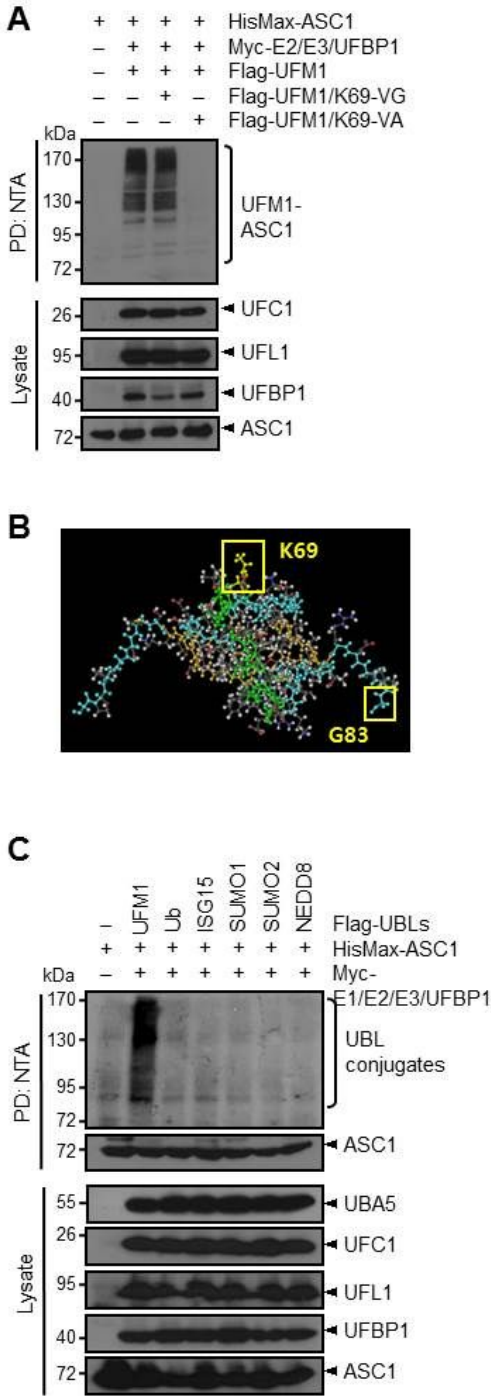
A
+ + + + HisMax-ASC1
– + + + Myc-E2/E3/UFBP1
– + + + Flag-UFM1
– – + – Flag-UFM1/K69-VG
– – – + Flag-UFM1/K69-VA
kDa
PD: NTA
170
130
95
72
UFM1-
ASC1
Lysate
26
95
40
72
UFC1
UFL1
UFBP1
ASC1
B
K69
G83
C
– UFM1 Ub ISG15 SUMO1 SUMO2 NEDD8
Flag-UBLs
+ + + + + + + HisMax-ASC1
kDa – + + + + + + Myc-
E1/E2/E3/UFBP1
PD: NTA
170
130
95
72
UBL
conjugates
72
ASC1
Lysate
55
26
95
40
72
UBA5
UFC1
UFL1
UFBP1
ASC1

4. Identification of the UFM1 acceptor sites in ASC1

To determine the UFM1 acceptor sites in ASC1, various deletion constructs were generated (Figure 18A). Of these, the constructs lacking the amino acids 300-370 (i.e., Δ3, Δ6, and Δ7) were not ufmylated upon expression in HEK293T cells with UFM1-conjugating system (Figure 18B). Since the deletion (300-370) has six Lys residues, I generated K-to-R mutations in various combinations (Figure 19A). Of these, replacement of Lys324, Lys325, Lys334, and Lys367 by Arg abrogated ASC1 ufmylation (Figure 19B), indicating that they are the ufmylation sites. Henceforth, the ufmylation-defective ASC1 mutant was referred to as 4KR. Endogenous ASC1 in HeLa cells has been shown to localize predominantly in the nucleus (Kim et al., 1999). Immunocytochemistry showed that the 4KR mutation has little or no effect on the nuclear localization of ASC1 in MCF7 cells (Figure 20).

Figure 18. Identification of UFM1 accepter site region in ASC1

(A and B) Deletions of ASC1 were generated, tagged with HisMax to their N-termini, and expressed in HEK293T cells with Flag-UFM1 and UFM1-conjugating system (A). Cell lysates were subjected to pull-down with NTA resins followed by immunoblot with anti-Flag antibody (B).

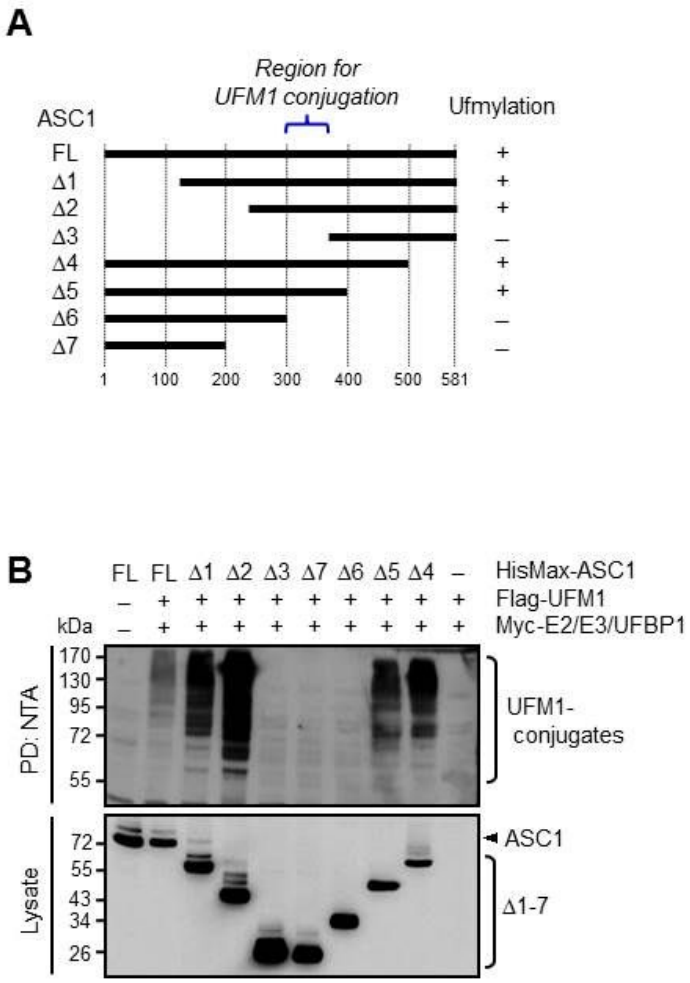
A
Region for
UFM1 conjugation
ASC1
Ufmylation
FL
Δ1
Δ2
Δ3
Δ4
Δ5
Δ6
Δ7
+
+
+
–
+
+
–
–
1
100
200
300
400
500
581
B
FL FL Δ1 Δ2 Δ3 Δ7 Δ6 Δ5 Δ4 –
HisMax-ASC1
– + + + + + + + + +
Flag-UFM1
kDa – + + + + + + + + +
Myc-E2/E3/UFBP1
PD: NTA
170
130
95
72
55
UFM1-
conjugates
Lysate
72
55
43
34
26
ASC1
Δ1-7

Figure 19. Identification of UFM1 accepter sites in ASC1

(A and B) The Lys residues in the amino acid sequence of 300-370 were replaced by Arg as indicated (A). The ASC1 mutants were then expressed (B).

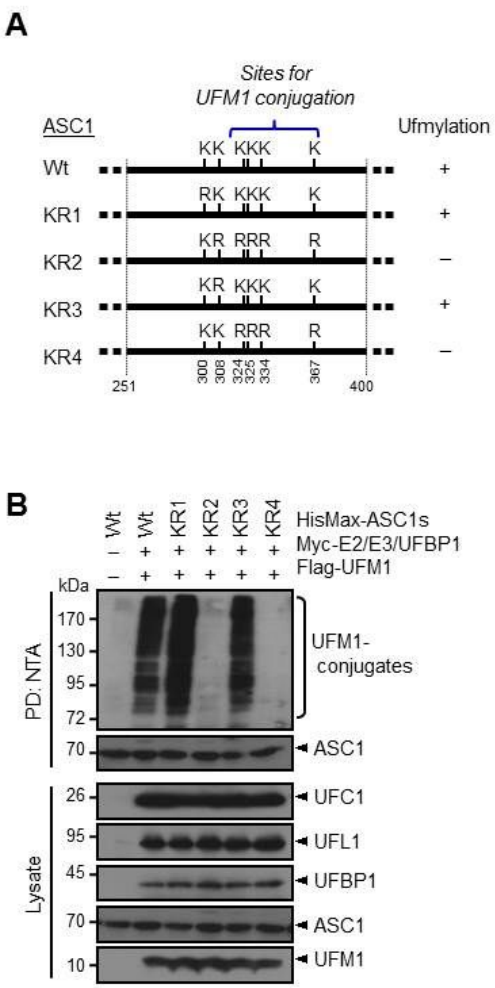
A
Sites for
UFM1 conjugation
ASC1
Ufmylation
Wt
KR1
KR2
KR3
KR4
KK KKK K
RK KKK K
KR RRR R
KR KKK K
KK RRR R
+
+
–
+
–
251
300
308
324
325
334
367
400
B
Wt
Wt
KR1
KR2
KR3
KR4
HisMax-ASC1s
Myc-E2/E3/UFBP1
Flag-UFM1
kDa
PD: NTA
170
130
95
72
70
UFM1-
conjugates
ASC1
Lysate
26
95
45
70
10
UFC1
UFL1
UFBP1
ASC1
UFM1

Figure 20. Localization of ASC1 and its 4KR mutant

HisMax-tagged ASC1 and its 4KR mutant were expressed in MCF7 cells. Cells were stained by anti-Xpress antibody, and subjected to confocal microscopy. Bar, 20 mm.

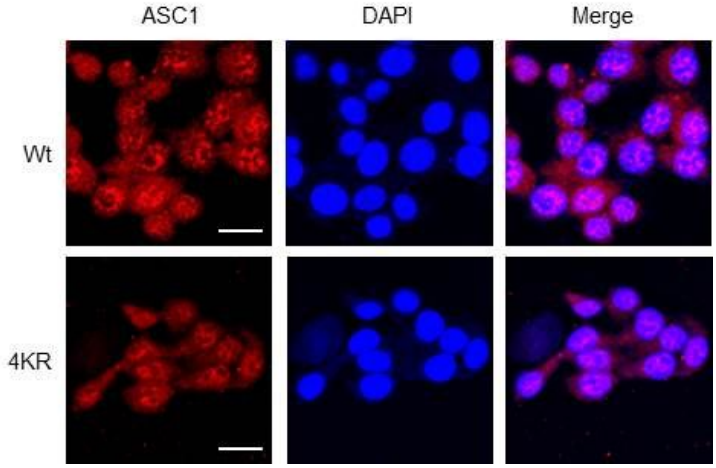
ASC1
DAPI
Merge
Wt
4KR

5. Reversal of ASC1 ufmylation by UfSP2

Our laboratory has previously identified two UFM1-specific proteases, UfSP1 and UfSP2 from rat (Kang et al., 2007). Unlike rat, human expresses only one functional UfSP2 enzyme. Therefore, I first examined whether human UfSP2 interacts with ASC1 by expressing them in HEK293T cells. Both UfSP2 and its catalytically inactive mutant (C302S), of which the active site Cys302 was replaced by Ser, bound to ASC1 (Figure 21A), indicating that the enzyme activity of UfSP2 is not required for its interaction with ASC1. In addition, the endogenous UfSP2 and ASC1 proteins could interact with each other (Figure 21B). To map the regions for binding between ASC1 and UfSP2, various deletions were generated and expressed in HEK293T cells. ASC1 bound to the region of amino acids 235-350 in UfSP2 (Figure 22A) and UfSP2 bound to the region of amino acids 125-200 in ASC1 (Figure 22B), which overlaps with the zinc-finger domain (Figure 22C).

Figure 21. UfSP2 interacts with ASC1

(A and B) Overexpressed HisMax-ASC1 and Flag-UfSP2 proteins (A) or their endogenous proteins in HEK293T cells (B) were immunoprecipitated with anti-Flag or anti-ASC1 antibody, respectively. CS denotes a catalytically inactive form of UfSP2.

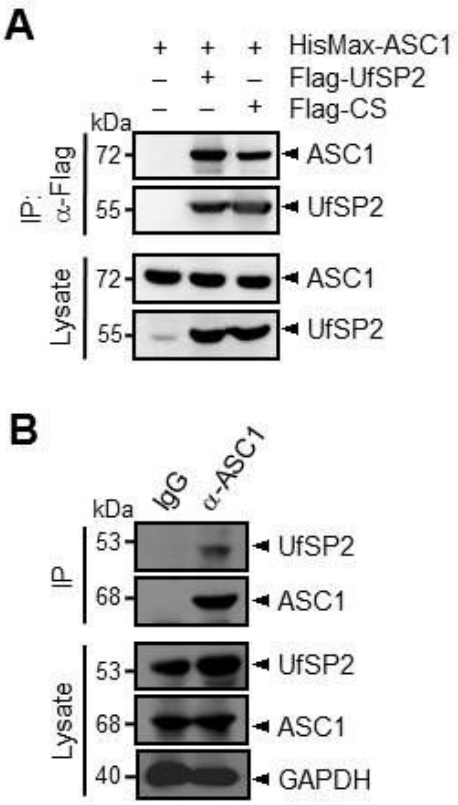
A
+ + + HisMax-ASC1
– + – Flag-UfSP2
– – + Flag-CS
kDa
IP: α-Flag
72
ASC1
55
UfSP2
Lysate
72
ASC1
55
UfSP2
B
IgG
α-ASC1
kDa
IP
53
UfSP2
68
ASC1
Lysate
53
UfSP2
68
ASC1
40
GAPDH

Figure 22. Identification of the regions for interaction between ASC1 and UfSP2

(A) Deletions of UfSP2 were generated, tagged with GFP to their N-termini, and expressed in HEK293T cells with HisMax-tagged ASC1. Cell lysates were subjected to pull-down with NTA-resins followed by immunoblot with anti-GFP or anti-Xpress antibody. (B) Deletions of ASC1 were generate, tagged with HisMax to their N-termini, and expressed in HEK293T cells with Flag-UfSP2. Cell lysates were subjected to pull-down with anti-Flag M2 antibody-conjugated resins followed by immunoblot with anti-Xpress or anti-Flag antibody. (C) Based on the data of (A and B) and Figure S1, the binding regions of UFL1, UFBP1, UfSP2, and nuclear receptors (NRs) within ASC1 were shown. ZF denotes the zinc finger domain.

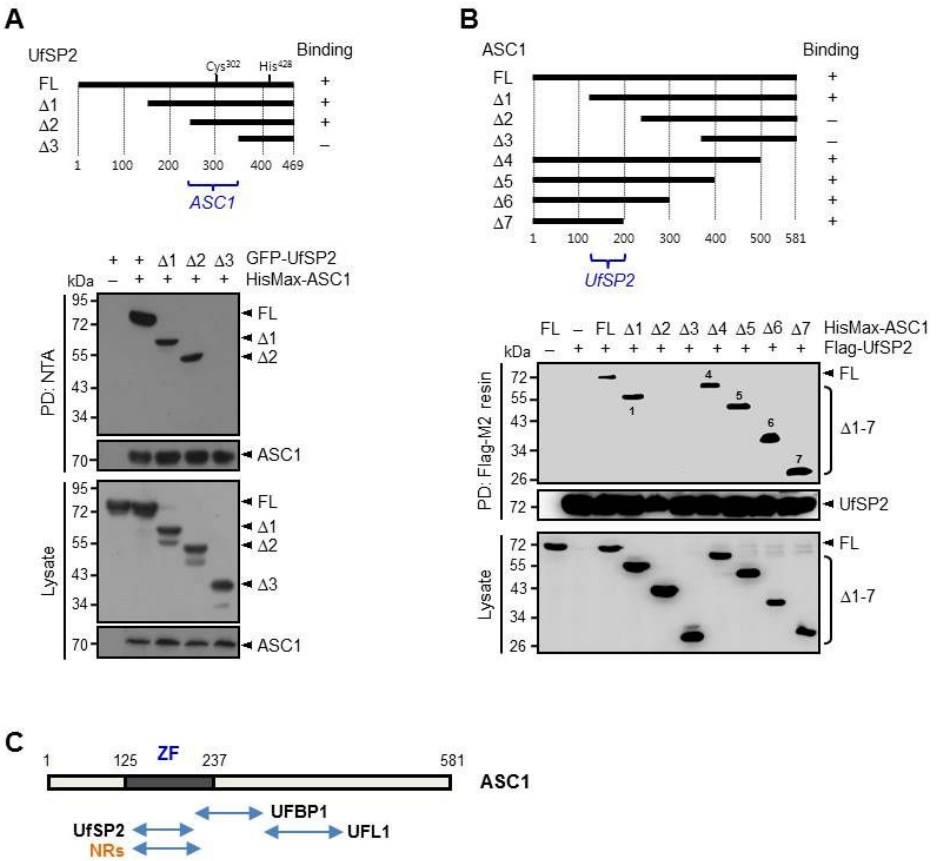
A
UfSP2
Binding
Cys302
His428
FL
Δ1
Δ2
Δ3
1
100
200
300
400
469
ASC1
+ + Δ1 Δ2 Δ3 GFP-UfSP2
kDa – + + + + HisMax-ASC1
PD: NTA
95
72
55
43
34
70
FL
Δ1
Δ2
ASC1
Lysate
Δ3
B
ASC1
Binding
Δ4
Δ5
Δ6
Δ7
500
581
UfSP2
FL – FL Δ1 Δ2 Δ3 Δ4 Δ5 Δ6 Δ7 HisMax-ASC1
Flag-UfSP2
PD: Flag-M2 resin
26
Δ1-7
UfSP2
C
125
ZF
237
581
UFBP1
UfSP2
UFL1
NRs

I next examined whether UfSP2 can remove UFM1 from ASC1. UfSP2, but not its inactive C302S mutant, eliminated poly-UFM1 chains from ASC1 (Figure 23A). Furthermore, expression of an UfSP2-specific shRNA (shUfSP2) led to a dramatic increase in the level of ufmylated ASC1 and this increase could be reversed by co-expression of the mouse form of UfSP2 (Figure 23B), which is insensitive to the shRNA. These results indicate that UfSP2 serves as a deufmylating enzyme for ASC1.

Figure 23. UfSP2 deufmylates ASC1 and UfSP2 knockdown promotes ASC1 ufmylation

(A) HisMax-ASC1 was expressed with UFM1-conjugating system in the presence and absence of UfSP2 or its CS mutant. Cell lysates were subjected to pull-down with NTA resins. (B) UfSP2 knockdown promotes ASC1 ufmylation. HisMax-ASC1 and UFM1-conjugating system were expressed with shNS and shUfSP2 in the presence or absence of Myc-mUfSP2, which is the mouse form of UfSP2.

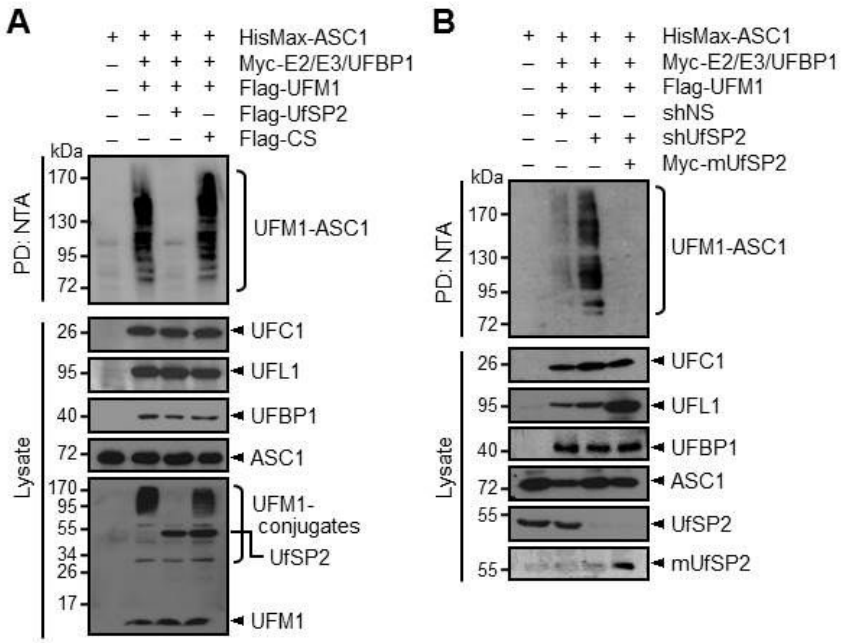
A
+ + + + HisMax-ASC1
– + + + Myc-E2/E3/UFBP1
– + + + Flag-UFM1
– – + – Flag-UfSP2
– – – + Flag-CS
kDa
PD: NTA
170
130
95
72
UFM1-ASC1
Lysate
26
95
40
72
UFC1
UFL1
UFBP1
ASC1
170
95
55
34
26
17
UFM1-
conjugates
UfSP2
UFM1
B
+ + + + HisMax-ASC1
– + + + Myc-E2/E3/UFBP1
– + + + Flag-UFM1
– + – – shNS
– – + + shUfSP2
– – – + Myc-mUfSP2
kDa
PD: NTA
170
130
95
72
UFM1-ASC1
Lysate
26
95
40
72
55
55
UFC1
UFL1
UFBP1
ASC1
UfSP2
mUfSP2

6. Requirement of E_2 for ASC1 ufmylation

Under in vitro conditions, ASC1 has been shown to interact with nuclear receptors, including ERα, in a ligand-independent manner (Kim et al., 1999). To determine whether ligands are required for the interaction of ASC1 with nuclear receptors in vivo, MCF7 cells were incubated with and without E_2. Immunoprecipitation analysis showed that the endogenous ASC1 and ERα proteins interacted with each other only in the presence of E_2 (Figure 24A). To investigate whether ufmylation of ASC1 also influences its interaction with ERα, MCF7 cells expressing ASC1 or its 4KR mutant were treated with E_2. Remarkably, the 4KR mutant, unlike wild-type ASC1, could not interact with ERα regardless of E_2 treatment (Figure 24B). Furthermore, co-expression of UfSP2 abrogated E2-induced interaction of ERα with ASC1 (Figure 24C). These results indicate that the interaction between ASC1 and ERα requires both the ligand binding to ERα and ASC1 ufmylation.

Figure 24. Requirement of E_2 for the binding of ASC1 to ERα

(A) E_2 induces the binding of ERα to ASC1. MCF7 cells were incubated with and without 100 nM E_2 for 1 h. They were then subjected to immunoprecipitation with anti-ASC1 (left) or anti-ERα antibody (right). (B) The 4KR mutation prevents E_2-mediated binding of ASC1 to ERα. ASC1 or its 4KR mutant was expressed in MCF7 cells with and without E_2. Cell lysates were subjected to pull-down with NTA resins (left) or immunoprecipitation with anti-ERα antibody (right). (C) UfSP2 blocks E_2-mediated binding of ASC1 to ERα. HisMax-ASC1 was expressed in MCF7 cells with UfSP2 in the presence or absence of E_2.

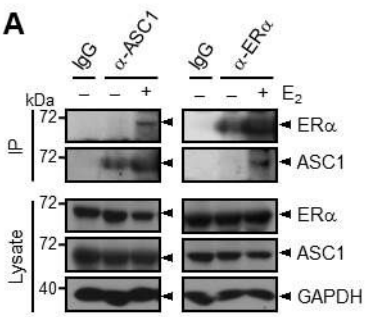
A
IgG
α-ASC1
IgG
α-ERα
– – + – – + E2
kDa
IP
72
72
ERα
ASC1
Lysate
72
72
40
ERα
ASC1
GAPDH

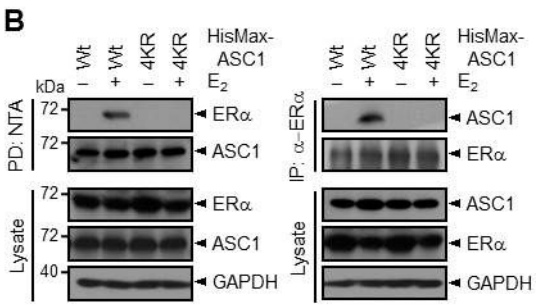
B
Wt Wt 4KR 4KR HisMax-ASC1
– + – + E2
kDa
PD: NTA
72
72
ERα
ASC1
Lysate
72
72
40
ERα
ASC1
GAPDH
IP: α-ERα
Wt Wt 4KR 4KR HisMax-ASC1
– + – + E2
ASC1
ERα
Lysate
ASC1
ERα
GAPDH

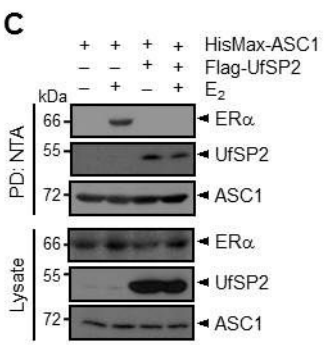
C
+ + + + HisMax-ASC1
– – + + Flag-UfSP2
– + – + E2
kDa
PD: NTA
66
55
72
ERα
UfSP2
ASC1
Lysate
66
55
72
ERα
UfSP2
ASC1

I next examined the effect of E_2 on ASC1 ufmylation. Intriguingly, ASC1 could be ufmylated only when cells were treated with E_2 (Figure 25A). E_2 showed little or no effect on expression of UFM1-conjugating system and UfSP2 (data not shown). Of note, however, was the finding that UfSP2 binds to the zinc-finger domain of ASC1 (Figure 22C), to which ERα binds (Kim et al., 1999), suggesting that E_2-bound ERα might compete with UfSP2 for binding to the zinc-finger domain of ASC1. Increased expression of UfSP2 caused a gradual decrease in the interaction between ERα and ASC1 (Figure 25B), while that of ERα led to a decrease in the binding between UfSP2 and ASC1 (Figure 25C). These results indicate that E_2-bound ERα and UfSP2 compete with each other for binding to ASC1. These results also suggest that without E_2, UfSP2 remains bound to ASC1 for preventing its ufmylation.

Figure 25. Requirement of E_2 for ASC1 ufmylation

(A) E_2 induces ASC1 ufmylation. MCF7 cells expressing Flag-UFM1 was incubated with and without E_2 followed by immunoprecipitation with anti-Flag and anti-ASC1 antibodies. (B and C) UfSP2 completes with ERα for binding to ASC1. Increasing amounts of UfSP2 (B) and ERα (C) were expressed in HEK293T cells with the fixed amounts of ERα and UfSP2, respectively.

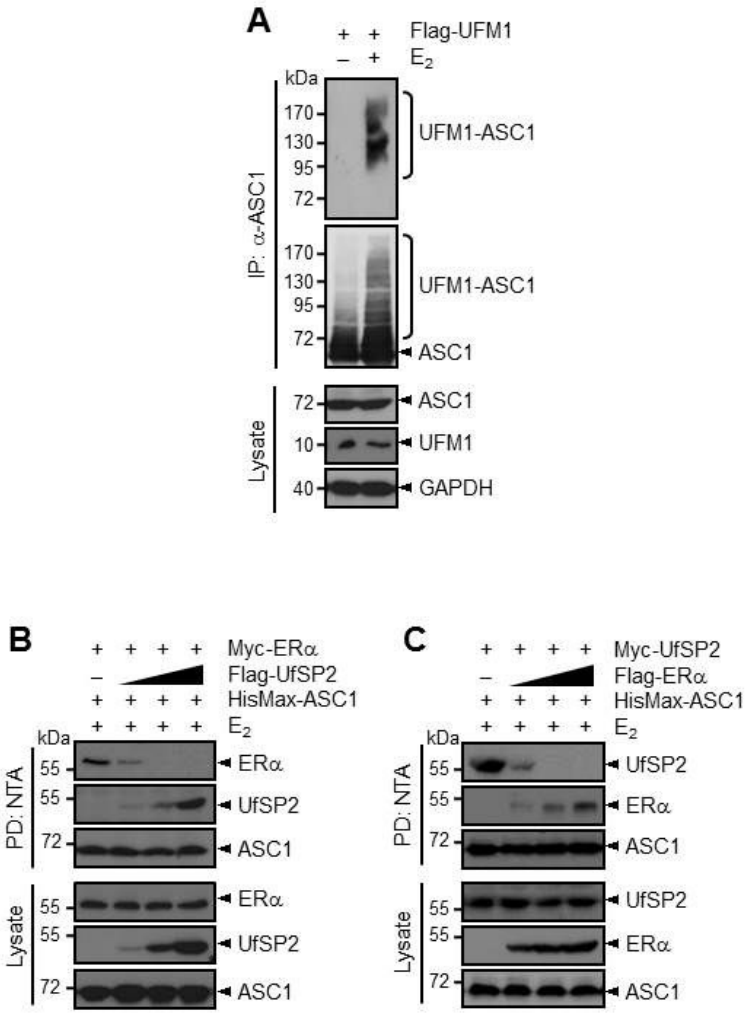
A
+ +
– +
Flag-UFM1
E2
kDa
170
130
95
72
UFM1-ASC1
170
130
95
72
UFM1-ASC1
ASC1
IP: α-ASC1
72
ASC1
10
UFM1
40
GAPDH
Lysate
B
+ + + +
– + + +
+ + + +
+ + + +
Myc-ERα
Flag-UfSP2
HisMax-ASC1
E2
kDa
55
ERα
55
UfSP2
72
ASC1
PD: NTA
55
ERα
55
UfSP2
72
ASC1
Lysate
C
+ + + +
– + + +
+ + + +
+ + + +
Myc-UfSP2
Flag-ERα
HisMax-ASC1
E2
kDa
55
UfSP2
55
ERα
72
ASC1
PD: NTA
55
UfSP2
55
ERα
72
ASC1
Lysate

To determine whether endogenous UfSP2 indeed blocks ufmylation of endogenous ASC1, shUfSP2 was expressed in MCF7 cells. Knockdown of UfSP2 in the absence of E_2 led to a marked increase in the level of ufmylated ASC1 (Figure 26), indicating that UfSP2 bound to ASC1 continuously deufmylates it. However, ERα could not interact with ufmylated ASC1 without E_2, again indicating that E_2 binding is required for the interaction of ERα with ASC1. These results also suggest that E_2-bound ERα displaces UfSP2 for binding to ASC1 and in turn allows ASC1 ufmylation, which further enhances the interaction between ASC1 and ERα.

Figure 26. UfSP2 knockdown leads to E_2-independent ASC1 ufmylation

Flag-UFM1 was expressed in MCF7 cells with shNS or shUfSP2 in the presence or absence of E_2.

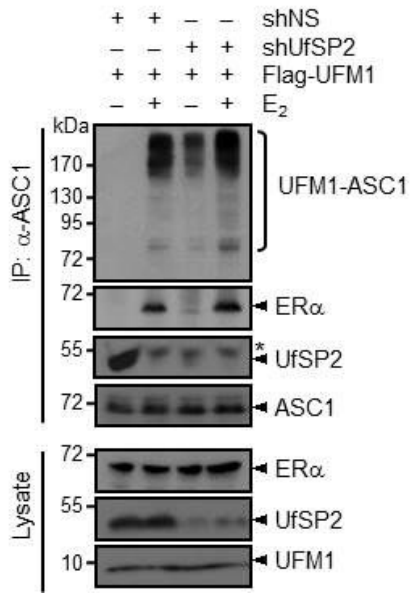
+ + – – shNS
– – + + shUfSP2
+ + + + Flag-UFM1
– + – + E2
kDa
170
130
95
72
UFM1-ASC1
IP: α-ASC1
72
ERα
55
*
UfSP2
72
ASC1
Lysate
72
ERα
55
UfSP2
10
UFM1

I next examined whether E_2 can also induce ASC1 ufmylation in other ERα-positive cells. E_2 treatment led to ASC1 ufmylation in ERα-positive BT-474 cells (Figure 27A), but not in ERα-negative MDA-MB-231 cells (Figure 27B). ASC1 also serves as a transcriptional co-activator of other nuclear receptors, such as AR (Kim et al., 1999; Lee et al., 1995; Xu et al., 2009). DHT, an AR agonist, induced ASC1 ufmylation in AR-positive LNCaP cells (Figure 27C), but not in AR-negative PC3 cells (Figure 27D). These results indicate that ligand-dependent ASC1 ufmylation is specific to cognate nuclear receptors.

Figure 27. Nuclear receptor ligand-specific ufmylation of ASC1

(A and B) Flag-UFM1 was expressed in ERα-positive BT-474 (A) and ERα-negative MDA-MB-231 cells (B). After incubation with and without E_2, cells were subjected to immunoprecipitation with anti-ASC1 antibody. (C and D) Flag-UFM1 was expressed in AR-positive LNCaP (C) and AR-negative PC3 cells (D). After incubation with and without DHT, cells were subjected to immunoprecipitation with anti-ASC1 antibody.

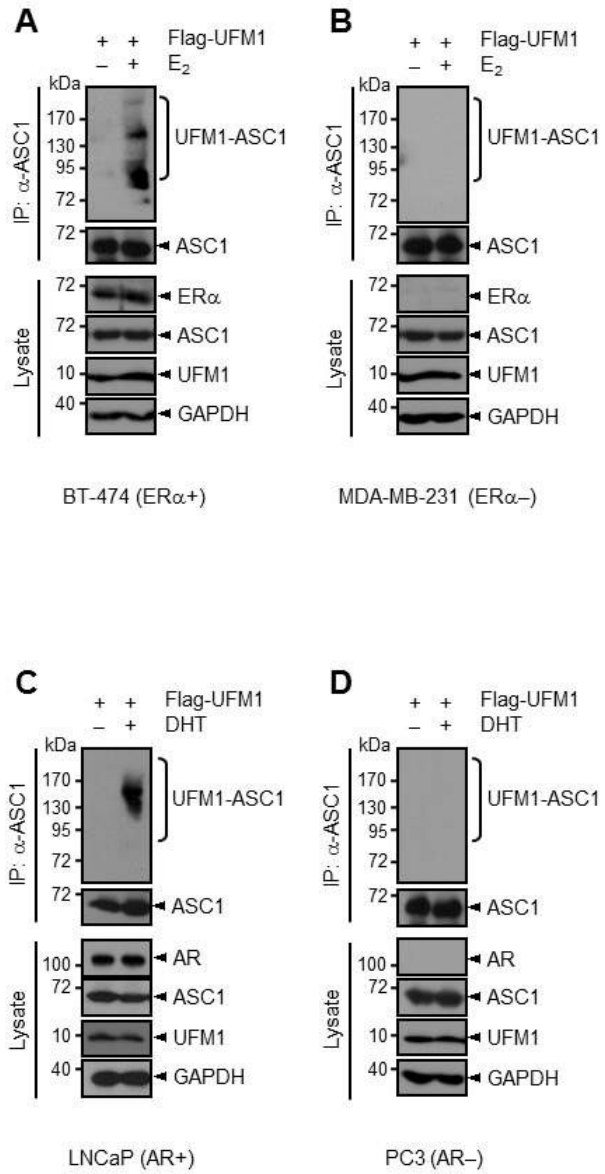
A
+ + Flag-UFM1
– + E2
kDa
170
130
95
72
72
IP: α-ASC1
UFM1-ASC1
ASC1
72
72
10
40
Lysate
ERα
ASC1
UFM1
GAPDH
BT-474 (ERα+)
B
+ + Flag-UFM1
– + E2
kDa
170
130
95
72
72
IP: α-ASC1
UFM1-ASC1
ASC1
72
72
10
40
Lysate
ERα
ASC1
UFM1
GAPDH
MDA-MB-231 (ERα–)
C
+ + Flag-UFM1
– + DHT
kDa
170
130
95
72
72
IP: α-ASC1
UFM1-ASC1
ASC1
100
72
10
40
Lysate
AR
ASC1
UFM1
GAPDH
LNCaP (AR+)
D
+ + Flag-UFM1
– + DHT
kDa
170
130
95
72
72
IP: α-ASC1
UFM1-ASC1
ASC1
100
72
10
40
Lysate
AR
ASC1
UFM1
GAPDH
PC3 (AR–)

7. Requirement of ASC1 ufmylation for recruitment of co-activators to ERE

For efficient ERα transactivation, other co-activators, including p300 and SRC1, need to be recruited to the ER-responsive elements (ERE) (Hanstein et al., 1996; Smith et al., 1996). To investigate the effect of ASC1 ufmylation on co-activator recruitment, I first examined the effect of 4KR mutation on the ability of ASC1 to bind p300 and SRC1. The interaction of ASC1 with p300 and SRC1 was increased upon E_2 treatment and this increase was abolished by the 4KR mutation (Figure 28A). Furthermore, UBA5 knockdown inhibited their interaction (Figure 28B), whereas UfSP2 knockdown promoted it (Figure 28C). These results suggest that poly-UFM1 chains conjugated to ASC1 serves as a scaffold for recruitment of p300 and SRC1.

Figure 28. Requirement of ASC1 ufmylation for recruitment of co-activators

(A and B) The 4KR mutation and UBA5 knockdown inhibit the interaction of ASC1 with p300 and SRC1. ASC1 or its 4KR mutant (A) and shNS or shUBA5 (B) were expressed in MCF7 cells in the presence or absence of 100 nM E_2. (C) UfSP2 knockdown promotes the interaction of ASC1 with p300 and SRC1. Cells expressing shNS or shUfSP2 were incubated with and without E_2.

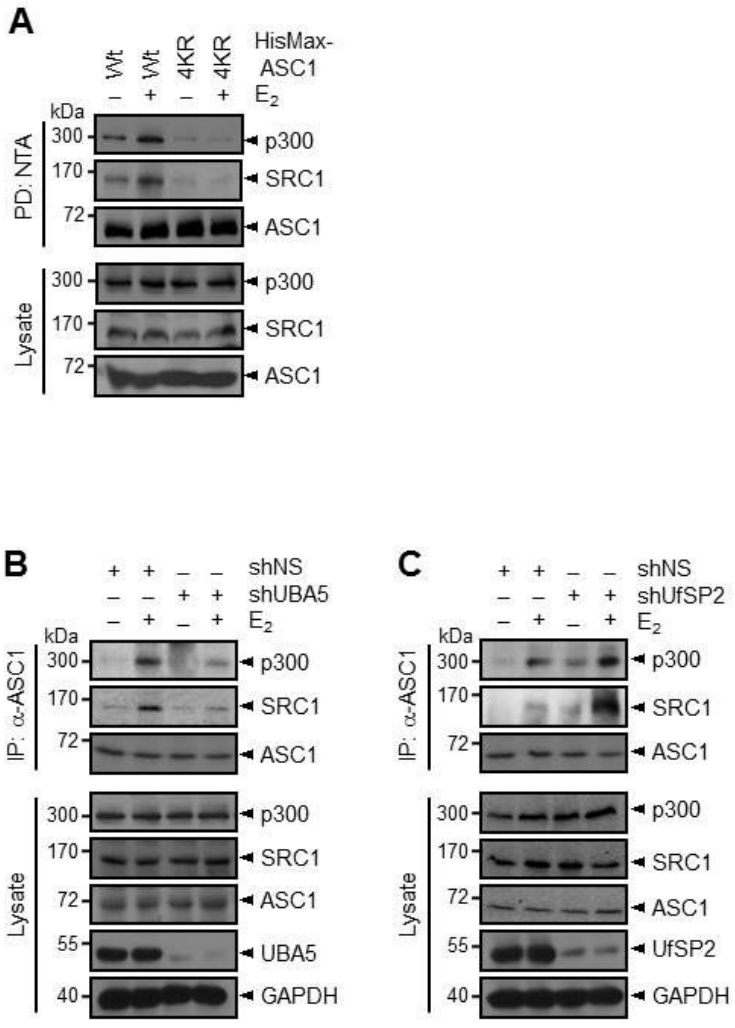
A
Wt
Wt
4KR
4KR
HisMax-ASC1
–
+
–
+
E2
kDa
PD: NTA
300
170
72
p300
SRC1
ASC1
Lysate
300
170
72
p300
SRC1
ASC1
B
+
+
–
–
shNS
–
–
+
+
shUBA5
–
+
–
+
E2
kDa
IP: α-ASC1
300
170
72
p300
SRC1
ASC1
Lysate
300
170
72
55
40
p300
SRC1
ASC1
UBA5
GAPDH
C
+
+
–
–
shNS
–
–
+
+
shUfSP2
–
+
–
+
E2
kDa
IP: α-ASC1
300
170
72
p300
SRC1
ASC1
Lysate
300
170
72
55
40
p300
SRC1
ASC1
UfSP2
GAPDH

I then examined the effect of ASC1 ufmylation on recruitment of ERα, p300, and SRC1 to the pS2 promoter by ChIP analysis. Whereas the 4KR mutation showed little or no effect on the recruitment of ERα to the promoter, it markedly decreased that of ASC1, SRC1, and p300 (Figure 29A). Furthermore, knockdown of UBA5, ASC1, or both dramatically reduced E_2-dependent recruitment of the co-activators (Figure 29B). In contrast, depletion of UfSP2 increased the recruitment of the co-activators and this increase was abrogated by co-knockdown of ASC1 (Figure 29C). These results indicate that ufmylation of ASC1 is required for recruitment of the co-activators and itself to the pS2 promoter.

Figure 29. Effect of ASC1 ufmylation on recruitment of ERα, p300, and SRC1 to the pS2 promoter

(A) The 4KR mutation inhibits the recruitment of ASC1, p300, and SRC1 to the pS2 promoter. HisMax-tagged ASC1 or its 4KR mutant was expressed in MCF7 cells. Cells were then subjected to ChIP analysis. (B and C) Knockdowns of UBA5 and UfSP2 inversely affect the recruitment of ASC1, p300, and SRC1 to the pS2 promoter. shUBA5 (B) or shUfSP2 (C) was expressed in MCF7 cells with and without shASC1. Data in (A-C) are the mean ± s.d. (n = 3).

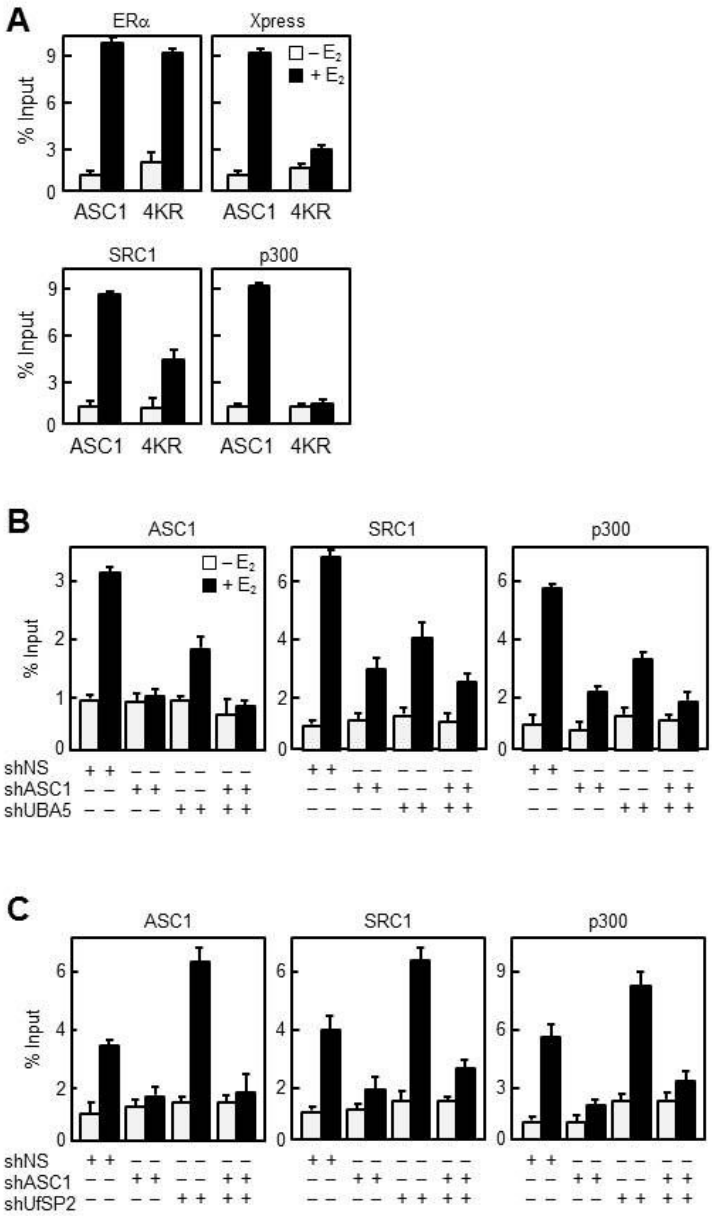
A
ERα
Xpress
% Input
□ – E2
■ + E2
ASC1 4KR ASC1 4KR
SRC1
p300
B
ASC1
SRC1
p300
shNS
shASC1
shUBA5
C
shUfSP2

8. Requirement of ASC1 ufmylation for E_2-induced ERα transactivation

I next examined whether ASC1 ufmylation is required for ERα transactivation by using a reporter vector ERE-Luc. Overexpression of ASC1 in the presence of E_2 led to an increase in the activity of ERα and this increase was further enhanced by co-expression of UFM1-conjugating system (Figure 30A). However, the 4KR mutation abolished the stimulatory effect of ASC1. Furthermore, knockdown of UBA5, ASC1, or both significantly reduced the ERα activity (Figure 30B), whereas that of UfSP2 increased it and this increase was abrogated by co-knockdown of ASC1 (Figure 30C). These results indicate that ASC1 ufmylation is required for ERα transactivation.

Figure 30. Effect of ASC1 ufmylation on E_2-induced ERα transactivation

(A and B) The 4KR mutation and UBA5 knockdown abrogate the transactivity of ERα. ASC1 or its 4KR mutant with UFM1-conjugating system (UFM-S) (A) and shNS or shUBA5 (B) were expressed in MCF7 cells in the presence or absence of E_2. Cells were also transfected with ERE-Luc. Cell lysates were then assayed for the luciferase activity. The activities seen with cells transfected with empty vectors were expressed as 1.0 and the others were as its relative values. (C) UfSP2 knockdown promotes the transactivity of ERα. Data in (A-C) are the mean ± s.d. (n = 3).

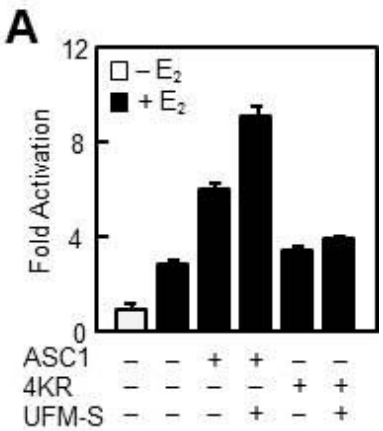
A
12
8
4
0
Fold Activation
– E_2
+ E_2
ASC1 – – + + – –
4KR – – – – + +
UFM-S – – – + – +

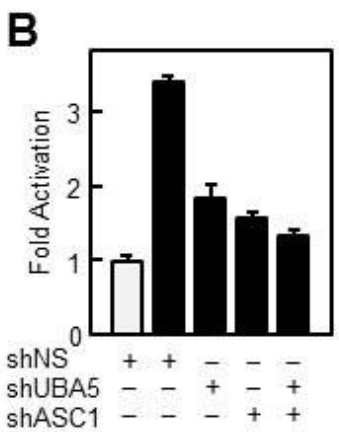
B
3
2
1
0
Fold Activation
shNS + + – – –
shUBA5 – – + – +
shASC1 – – – + +

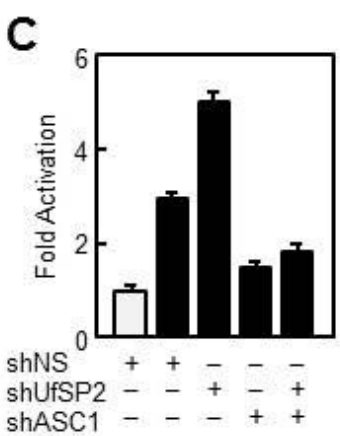
C
6
4
2
0
Fold Activation
shNS + + – – –
shUfSP2 – – + – +
shASC1 – – – + +

To determine whether ASC1 ufmylation is indeed required for transcriptional activation of ERα target genes, I measured the mRNA levels of pS2, cyclin D1, and c-Myc. Overexpression of ASC1 led to a significant increase in all of their mRNA levels and this increase was abolished by the 4KR mutation (Figure 31A). Furthermore, knockdown of UBA5, ASC1, or both reduced their mRNA levels (Figure 31B), whereas that of UfSP2 increased them and this increase was abrogated by co-knockdown of ASC1 (Figure 31C). Collectively, these results indicate that ASC1 ufmylation is crucial for ERα transactivation.

Figure 31. Effect of ASC1 ufmylation on ERα target genes

(A) The 4KR mutation of ASC1 abrogates the expression of ERα target genes. ASC1 or its 4KR mutant was expressed in MCF7 cells. The transcript levels of pS2, cyclin D1, and c-Myc were determined by qPCR. (B and C) Knockdowns of UBA5 and UfSP2 inversely affect the expression of ERα target genes. shUBA5 (B) or shUfSP2 (C) was expressed in MCF7 cells with and without shASC1. Data in (A-C) are the mean ± s.d. (n = 3).

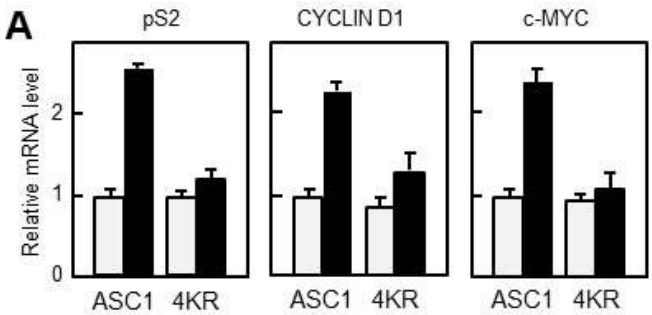
A
pS2
CYCLIN D1
c-MYC
Relative mRNA level
0
1
2
ASC1 4KR
ASC1 4KR
ASC1 4KR

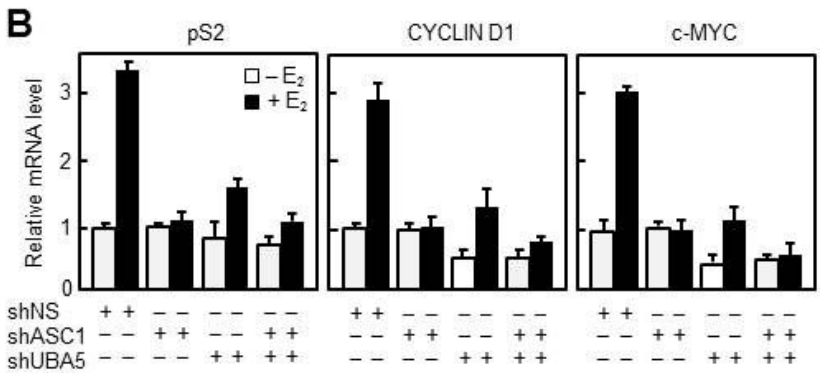
B
pS2
CYCLIN D1
c-MYC
□ – E2
■ + E2
Relative mRNA level
0
1
2
3
shNS + + – – – – – – + + – – – – + + – – – –
shASC1 – – + + – – + + – – + + – – + + – – + +
shUBA5 – – – – + + + + – – – – + + + + – – – – + + + +

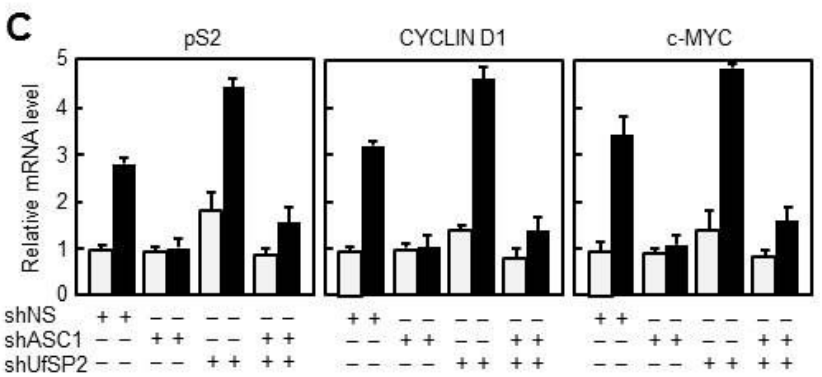
C
pS2
CYCLIN D1
c-MYC
Relative mRNA level
0
1
2
3
4
5
shNS + + – – – – – – + + – – – – + + – – – –
shASC1 – – + + – – + + – – + + – – + + – – + +
shUfSP2 – – – – + + + + – – – – + + + + – – – – + + + +

9. Promotion of cell growth and tumor formation by ASC1 ufmylation

Nearly 70% of breast cancer is ERα-positive (Jozwik and Carroll, 2012). To determine whether ASC1 ufmylation is involved in development of ERα-positive breast tumors, I first examined the effect of ASC1 overexpression on the ability of MCF7 cells in anchorage-independent colony formation. ASC1 expression significantly increased the number of colonies in the absence of E_2 and this effect was further enhanced in its presence (Figures 32A and 32B). However, the 4KR mutation abrogated the increases in colony formation. Furthermore, knockdown of UBA5, ASC1, or both decreased the ability of MCF7 cells to form colonies, whereas knockdown of UfSP2 dramatically increased it and this increase was abrogated by co-knockdown of ASC1 (Figures 33A and 33B). Similar effects on cell proliferation were observed upon knockdown of UBA5 or UfSP2 with and without ASC1, as analyzed by colorimetric MTT assay (Figure 34). Note that for the experiments in Figure 32 (also for Figures 36 and 37: see below), endogenous ASC1 was depleted by stable expression of shASC1 in MCF7 cells and then shASC1-insensitive ASC1 and 4KR

were overexpressed (Figure 35A). Figure 35B shows the expression of endogenous ASC1, UBA5, and UfSP2 proteins in MCF7 cells used in Figure 33. These results indicate that ASC1 ufmylation accelerates cell growth.

Figure 32. Promotion of E_2-mediated colony formation by ASC1 ufmylation

(A) The 4KR mutation of ASC1 aboragtes colony formation. MCF7 cells expressing ASC1 or its 4KR mutant were grown on soft agar in the presence or absence of E_2. After incubation for 5 weeks, colonies were stained with crystal violet. (B) Experiments were performed as in (A), and the numbers of colonies per plate were determined.

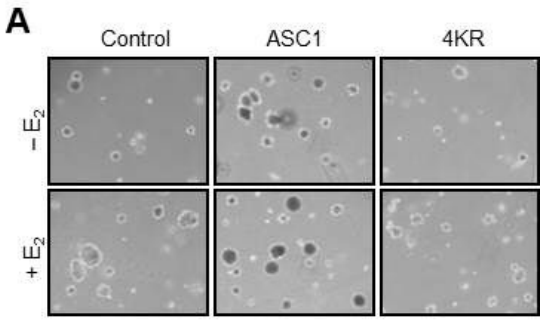
A
Control
ASC1
4KR
– E2
+ E2

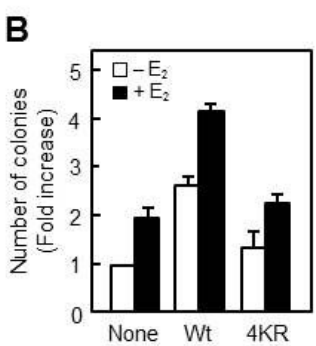
B
Number of colonies
(Fold increase)
– E2
+ E2
0
1
2
3
4
5
None
Wt
4KR

Figure 33. Knockdowns of UBA5 and UfSP2 inversely affect colony formation

(A) shUBA5 or shUfSP2 was expressed in MCF7 cells with and without shASC1. (B) Experiments were performed as in (A), and the numbers of colonies per plate were determined.

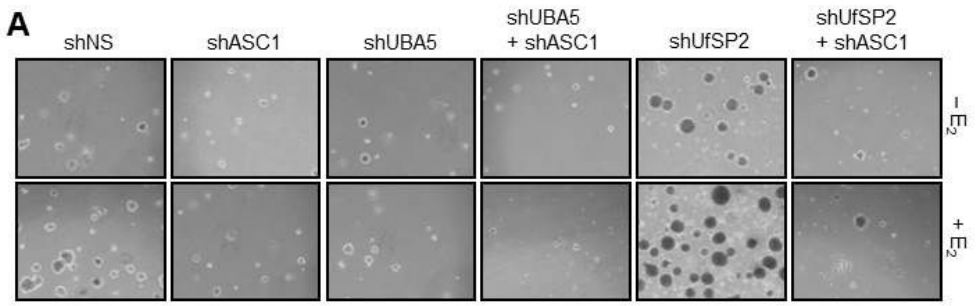
A
shNS
shASC1
shUBA5
shUBA5
+ shASC1
shUfSP2
shUfSP2
+ shASC1
– E2
+ E2

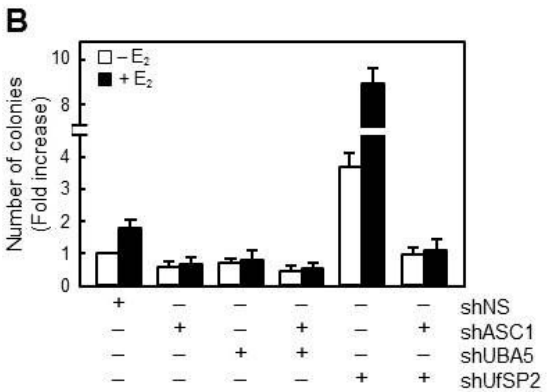
B
□ – E2
■ + E2
Number of colonies
(Fold increase)
10
8
4
3
2
1
0
shNS
shASC1
shUBA5
shUfSP2

Figure 34. Effects on cell proliferation upon knockdown of UBA5 or UfSP2 with and without ASC1

shUBA5 or shUfSP2 was expressed in MCF7 cells with and without shASC1. Cells were then subjected to MTT assay.

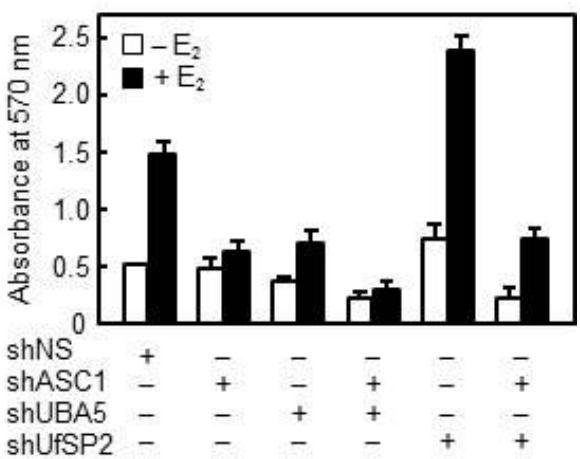
Absorbance at 570 nm
2.5
2.0
1.5
1.0
0.5
0
– E2
+ E2
shNS + – – – – –
shASC1 – + – + – +
shUBA5 – – + + – –
shUfSP2 – – – – + +

Figure 35. Immunoblot analysis for overexpression of ASC1 and its 4KR mutant and knockdown of ASC1, UBA5, and UfSP2

(A) Lysates obtained from cells in Figure 32 were subjected to immunoblot analysis. iASC1 and i4KR denote shASC1-insensitive ASC1 and its 4KR mutant, respectively, and eASC1 indicates endogenous ASC1. (B) Lysates obtained from cells in Figure 33 were subjected to immunoblot analysis.

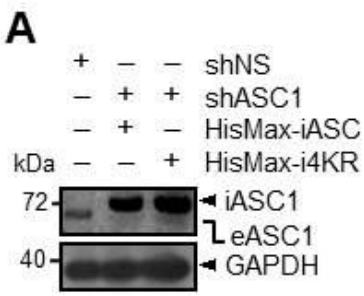
A
+ – – shNS
– + + shASC1
– + – HisMax-iASC
kDa – – + HisMax-i4KR
72
iASC1
eASC1
40
GAPDH

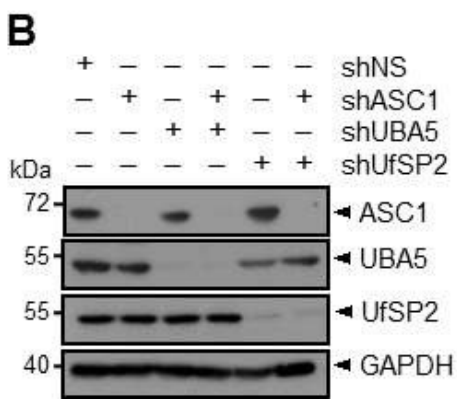
B
+ – – – – – shNS
– + – + – + shASC1
– – + + – – shUBA5
kDa – – – – + + shUfSP2
72
ASC1
55
UBA5
55
UfSP2
40
GAPDH

Using xenograft analysis, I next examined whether ASC1 ufmylation contributes to tumor formation in vivo. BALB/c nude mice injected with MCF7 cells expressing ASC1 developed significantly larger tumors than those with cells transfected with an empty vector even in the absence of E_2 (Figures 36A, 36B, and 36C). While the tumor sizes of MCF7-ASC1 xenografts further increased upon E_2 treatment, those of MCF7-4KR xenografts remained much smaller. Furthermore, mice injected with cells that stably express shASC1 or shUBA5 developed significantly smaller tumors than those with cells expressing shNS regardless of E_2 treatment (Figures 37A, 37B, and 37C). In contrast, shUfSP2 xenografts developed much larger tumors in the absence of E_2 and the tumor sizes were further increased in its presence as compared to those of shNS xenografts. However, the effect of UfSP2 knockdown on tumor growth was abrogated in mice injected with cells expressing both shUfSP2 and shASC1. These results indicate that ASC1 ufmylation is critical for E_2-mediated tumor growth.

Figure 36. The 4KR mutation prevents tumor growth

(A) BALB/c mice were injected with MCF7 cells stably expressing ASC1 or its 4KR mutant. Eight weeks after injection, mice were sacrificed, photographed, and dissected out of their tumors. (B) Tumor volumes were determined at each of indicated times after injection. (C) Their weights were measured. Control indicates the cells transfected with an empty vector. Data in (B and C) are the mean ± s.d. (n = 5).

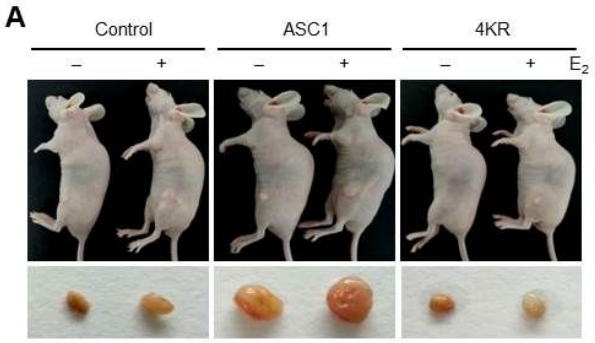
A
Control
ASC1
4KR
–
+
–
+
–
+
E2

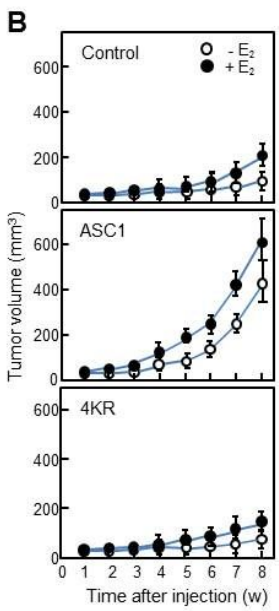
B
Control
- E2
+ E2
ASC1
4KR
Tumor volume (mm3)
0
200
400
600
0 1 2 3 4 5 6 7 8
Time after injection (w)

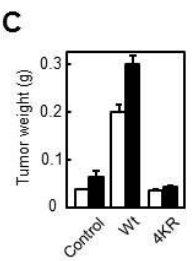
C
Tumor weight (g)
0
0.1
0.2
0.3
Control
Wt
4KR

Figure 37. Knockdowns of UBA5 and UfSP2 inversely affect tumor growth

(A) BALB/c mice were injected with MCF7 cells that stably express shUBA5 or shUfSP2 with and without shASC1. Eight weeks after injection, mice were sacrificed, photographed, and dissected out of their tumors. (B) Tumor volumes and weights were determined. (C) Their weights were measured. Control indicates the cells transfected with an empty vector. Data in (B and C) are the mean ± s.d. (n = 5).

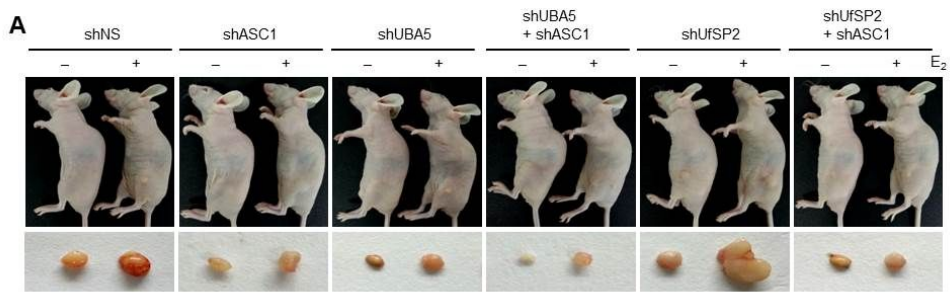
A
shNS
shASC1
shUBA5
shUBA5
+ shASC1
shUfSP2
shUfSP2
+ shASC1
– + – + – + – + – + – + E2

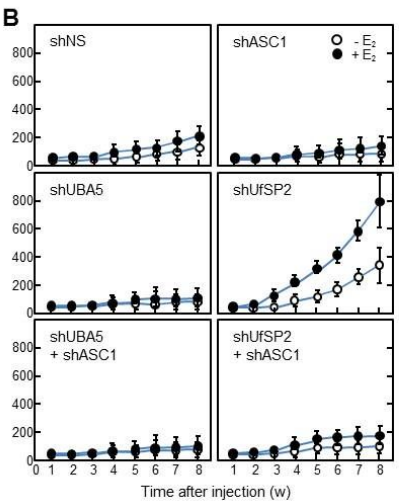
B
shNS
shASC1
shUBA5
shUfSP2
shUBA5
+ shASC1
shUfSP2
+ shASC1
- E2
+ E2
0 200 400 600 800
0 1 2 3 4 5 6 7 8
Time after injection (w)

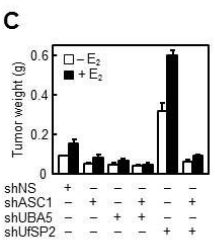
C
Tumor weight (g)
0 0.2 0.4 0.6
– E2
+ E2
shNS + – – – – –
shASC1 – + – + – +
shUBA5 – – + + – –
shUfSP2 – – – – + +

10. Up-regulation of the UFM1 system in breast cancer cell lines and tissues

To determine whether breast cancer is indeed associated with ASC1 ufmylation, I compared the expression of the UFM1 system in normal and breast cancer cells. Both the protein and mRNA levels of the UFM1 system in ERα-positive MCF7 and BT-474 cells were much higher than those in normal MCF10A cells and ERα-negative MDA-MB-231 cells (Figures 38A and 38B). Immunocytochemical analysis also revealed that expression of all components of the UFM1 system was up-regulated in MCF7 cells as compared to that in MCF10A cells (Figure 39), implicating a crucial role of the UFM1 system in ERα-positive breast cancer development. Interestingly, the level of ASC1, but not the other components, in MDA-MB-231 cells was significantly higher than that in MCF10A cells, suggesting a possibility that ASC1 may also be involved in ERα-negative breast cancer. Surprisingly, the expression of UfSP2 was also up-regulated in MCF7 and BT-474 cells, although to a lesser extent than the other components of the UFM1 system. Since UfSP2 plays an essential role in generation of matured UFM1 from its precursor in addition to its role in reversal of

ufmylation process, a moderate increase in UfSP2 level might be required for efficient ASC1 ufmylation.

Figure 38. Up-regulation of the UFM1 system in breast cancer cell lines

(A and B) The UFM1 system is up-regulated in ERα-positive breast cancer cell lines. (A) Cell lysates were subjected to immunoblot analysis. (B) Total RNAs were subjected to qPCR. Data are the mean ± s.d. (n = 3).

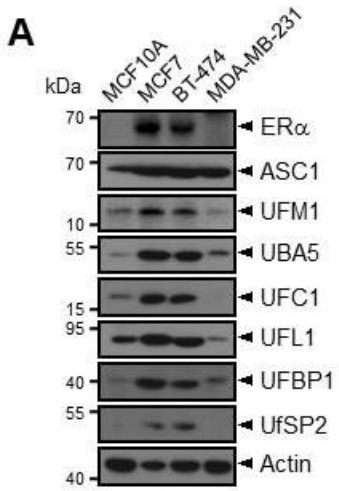
A
kDa
MCF10A
MCF7
BT-474
MDA-MB-231
70
ERα
70
ASC1
10
UFM1
55
UBA5
15
UFC1
95
UFL1
40
UFBP1
55
UfSP2
40
Actin

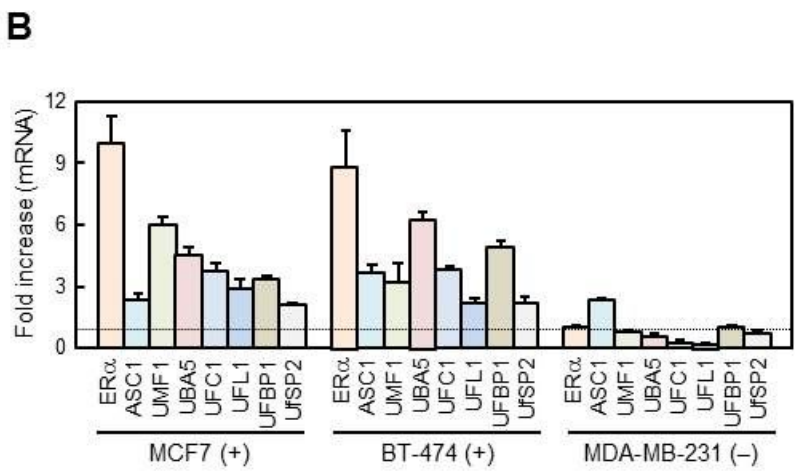
B
Fold increase (mRNA)
12
9
6
3
0
ERα
ASC1
UMF1
UBA5
UFC1
UFL1
UFBP1
UfSP2
MCF7 (+)
BT-474 (+)
MDA-MB-231 (–)

Figure 39. Immunocytochemical analysis of the UFM1 system in mammary cells

MCF10A (normal), MCF7 (ERα-positive), and MDA-MB-231 (ERα-negative) cells were subjected to immunocytochemistry. Bar, 50 mm.

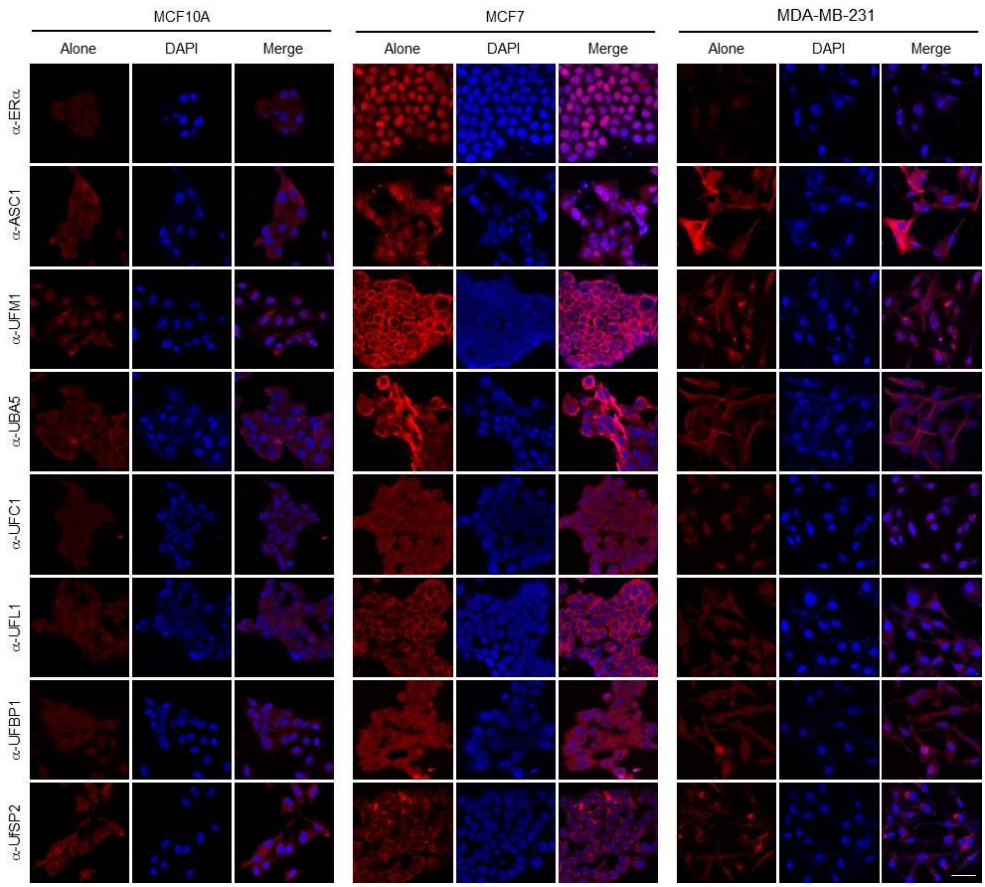
MCF10A
MCF7
MDA-MB-231
Alone
DAPI
Merge
α-ERα
α-ASC1
α-UFM1
α-UBA5
α-UFC1
α-UFL1
α-UFBP1
α-Ufsp2

The expression pattern of the UFM1 system, including UfSP2, in human breast tumor tissues (Figures 40 and 41) was remarkably similar to that of the cancer cell lines tested (Figures 38 and 39). Immunohistochemical analyses also showed that expression of all components of the UFM1 system was up-regulated in ERα-positive tumors as compared to that in normal tissues (Figure 42). Surprisingly, however, the protein level of UFM1 in ERα-positive tumors was similar to that in normal tissues or ERα-negative tumors (Figure 40A), despite the finding that its mRNA level was dramatically up-regulated in ERα-positive tumors (Figure 40B), consistent with its elevated expression in their tissue sections (Figures 41 and 42). While UFM1 seen in the SDS-PAGE gels represents its monomeric form, UFM1 detected by immunocytochemical and immunohistochemical analyses should represent both the free and conjugated forms. Since expression of all components of the UFM1-conjugating machinery was up-regulated in ERα-positive tumors, a large portion of elevated free UFM1 pool might have been conjugated to cellular proteins in addition to ASC1. Collectively, these results indicate that ASC1 ufmylation plays a crucial role

in ERα-positive breast cancer development.

Figure 40. Up-regulation of the UFM1 system in breast cancer tissues

(A) Tissue lysates were subjected to immunoblot analysis. (B) Total RNAs were subjected to qPCR. 'N' and 'T' denote normal and tumor tissues, respectively. Data are the mean ± s.d. (n = 7).

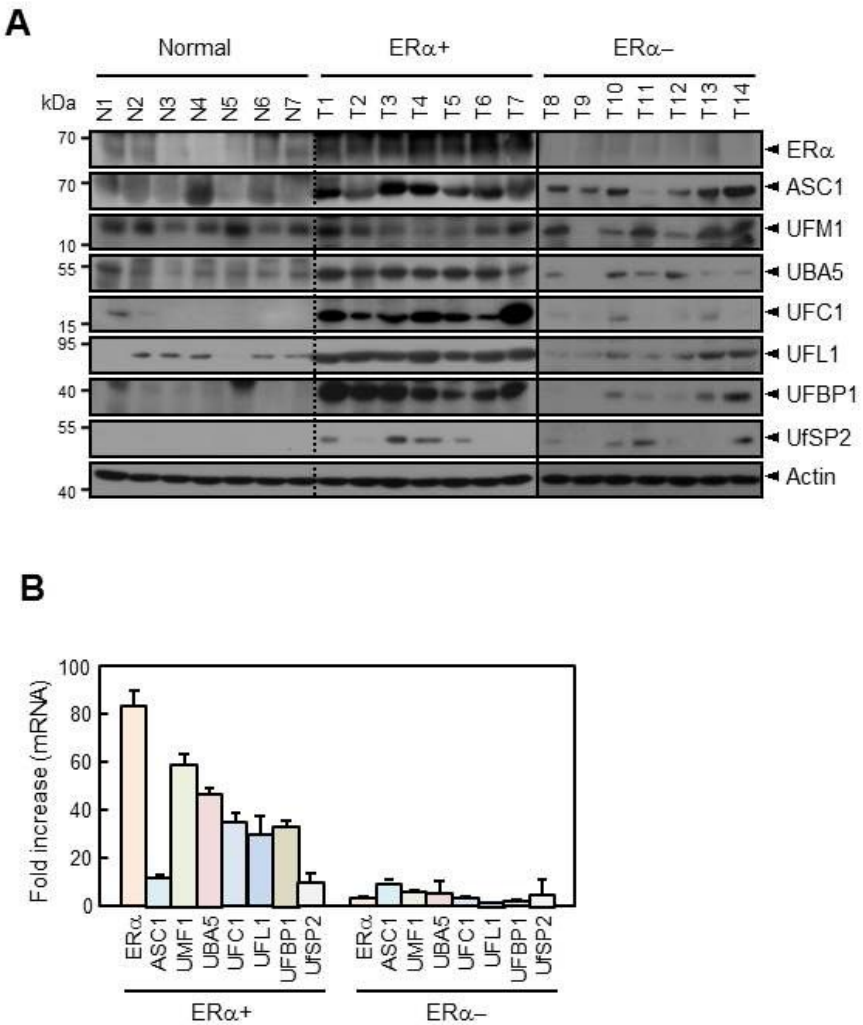
A
Normal
ERα+
ERα–
kDa
N1 N2 N3 N4 N5 N6 N7 T1 T2 T3 T4 T5 T6 T7 T8 T9 T10 T11 T12 T13 T14
70
70
10
55
15
95
40
55
40
ERα
ASC1
UFM1
UBA5
UFC1
UFL1
UFBP1
UfSP2
Actin
B
Fold increase (mRNA)
100
80
60
40
20
0
ERα ASC1 UMF1 UBA5 UFC1 UFL1 UFBP1 UfSP2
ERα+
ERα ASC1 UMF1 UBA5 UFC1 UFL1 UFBP1 UfSP2
ERα–

Figure 41. Immunocytochemical analysis of the UFM1 system in breast cancer tissues

Tissue sections were subjected to immunocytochemical analysis. The large boxes (bar, 50 μm) show the magnified view of the small boxes (bar, 20 μm).

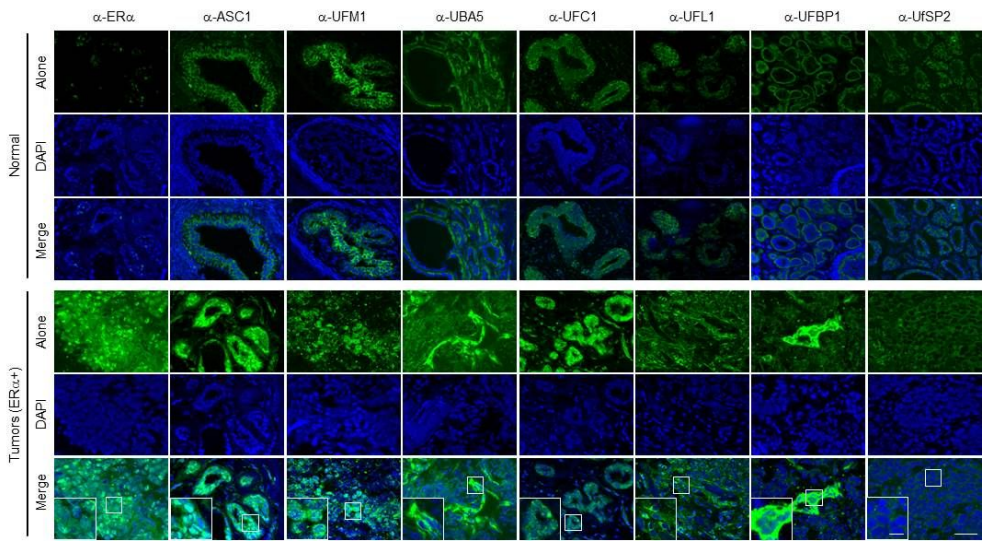
α-ERα
α-ASC1
α-UFM1
α-UBA5
α-UFC1
α-UFL1
α-UFBP1
α-UfSP2
Normal
Alone
DAPI
Merge
Tumors (ERα+)
Alone
DAPI
Merge

Figure 42. Immunohistochemcial analysis of the UFM1 system in normal and breast tumor tissues

Normal and ERα-positive tumor tissues were subjected to immunohistochemical analysis. The large boxes (bar, 30 μm) show the magnified view of the small boxes (bar, 20 μm).

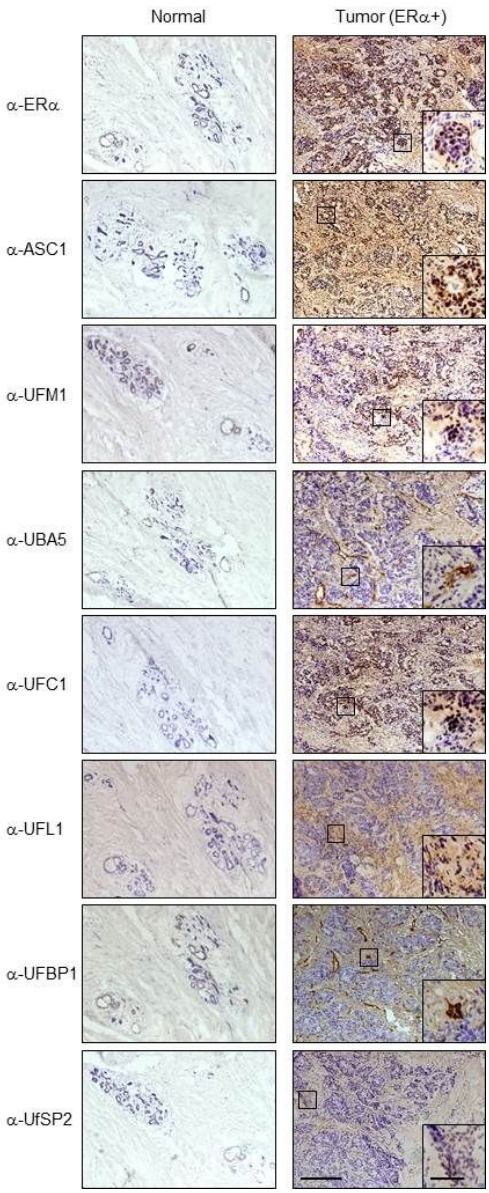
Normal
Tumor (ERα+)
α-ERα
α-ASC1
α-UFM1
α-UBA5
α-UFC1
α-UFL1
α-UFBP1
α-UfSP2

DISCUSSION

Based on the present findings, I propose a model for the role of ASC1 ufmylation in ERα-positive breast cancer development. In the absence of E_2, ASC1 can be modified by UFM1 by the sequential action of UBA5 (E1), UFC1 (E2), and UFL1 (E3) with UFBP1. However, this process appears to be rapidly reversed by UfSP2, which is bound to the zinc-finger domain of ASC1 (Figure 43A). In its presence, ERα displaces UfSP2 for binding to the zinc-finger domain and in turn allows ASC1 ufmylation by the UFM1-conjugating machinery. Poly-UFM1 chains formed on ASC1 then serve as a scaffold that recruits p300, SRC1, and itself to ERE in the promoters of ERα target genes via the DNA-binding domain of the receptor for their transcriptional activation. Consequently, ERα target gene products, including pS2, cyclin D1, and c-Myc, would be expressed and promote excessive cell proliferation, which leads to tumor formation (Figure 43B).

Figure 43. A model for the role of ASC1 ufmylation in ERα-positive breast cancer development

(A) Like ubiquitination, ufmylation of target proteins, including ASC1, is catalyzed by 3-step enzyme system consisting of UBA5 (E1), UFC1 (E2), and UFL1. Unlike ubiquitination, however, protein ufmylation requires an additional component, UFBP1. This ufmylation process can be reversed by the UFM1-specific protease UfSP2 in human cells. '~' indicates the thiosester linkage.

(B) In the absence of E_2, UfSP2 is bound to ASC1 to prevent ufmylation. In its presence, ERα displaces UfSP2 for binding to ASC1 and allows ASC1 ufmylation. Poly-UFM1 chains conjugated to ASC1 then recruit p300, SRC1, and itself to the promoters of ERα target genes for transcriptional activation, which leads to breast cancer development.

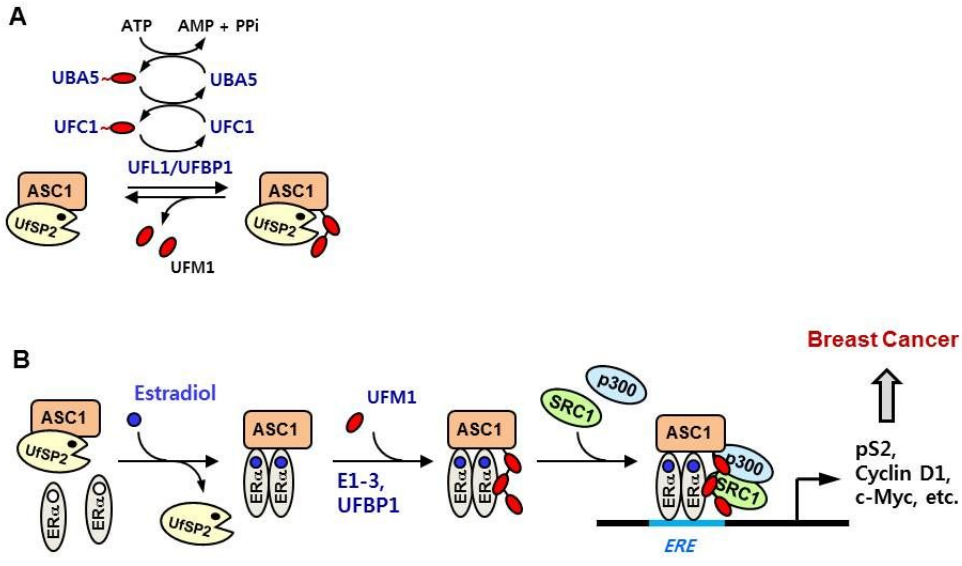
A
ATP
AMP + PPi
UBA5
UBA5
UFC1
UFC1
UFL1/UFBP1
ASC1
UfSP2
ASC1
UfSP2
UFM1
B
Breast Cancer
ASC1
UfSP2
Estradiol
ERα
ERα
ASC1
UfSP2
UFM1
E1-3,
UFBP1
ASC1
ERα
ERα
p300
SRC1
ASC1
ERα
ERα
p300
SRC1
pS2,
Cyclin D1,
c-Myc, etc.
ERE

Collectively, E_2-induced ASC1 ufmylation plays a critical role in breast cancer development by promoting transactivation. Of note was the findings that UFBP1 (C20orf116) serves as an essential cofactor in ASC1 ufmylation and that ufmylation of UFBP1 itself is required for ASC1 ufmylation. Since ufmylation of UFBP1 dramatically increases its affinity to the UFL1 E3 ligase, but not to ASC1, UFBP1 may first act as a substrate of UFL1 through their weak binding and the ufmylated UFBP1 then binds to the ligase with high affinity, which might be required for the activation of UFL1.

An unanswered question is where in cells ASC1 is modified by UFM1. This question arises from the subcellular locality of the UFM1 system: UFC1 mainly in the nucleus; UFM1 and UfSP2 in both the nucleus and the cytoplasm; UBA5, UFL1, and UFBP1 mainly in the cytoplasm and/or in the endoplasmic reticulum (Ha et al., 2011; Tatsumi et al., 2010). Moreover, UFBP1 has a putative signal sequence, suggesting that a portion of it may be embedded in the endoplasmic reticulum membrane. Notably, it has been shown that serum deprivation results in translocation of nuclear

ASC1 to the cytoplasm and this translocation can be reversed by supplement of serum or 9-cis-retinoic acid, a ligand of the RXR nuclear receptor (Kim et al., 1999). These findings suggest that ASC1 may be ufmylated in the cytoplasm and then translocated to the nucleus. However, ASC1 in MCF7 cells, unlike that in MCF10A cells and normal mammary tissues, resided mainly in the nucleus (Figures 39 and 41), and could be ufmylated only when treated with E_2 (Figure 25A). Moreover, the 4KR mutation, which abrogates ASC1 ufmylation, showed little or no effect on the locality of ASC1 (Figure 20). Interestingly, it has been reported that treatment with TSA, an inhibitor of HDAC, causes the release of UFBP1 from the endoplasmic reticulum and subsequent translocation to the nucleus (Neziri et al., 2010). However, treatment with E_2 did not show any effect on the locality of UFBP1 or ASC1 (data not shown). Thus, it remains unclear where ASC1 is ufmylated in cells.

ASC2 (also called AIB3), whose gene is amplified in breast cancer (Lee et al., 1999; Mahajan and Samuels, 2005, 2008), is capable of interacting with most, if not all, of the proteins that bind to ASC1. It also serves as a co-activator of nuclear

receptors (Caira et al., 2000; Ko et al., 2000; Lee et al., 1999; Mahajan and Samuels, 2000). However, ASC1 and ASC2 share little or no sequence homology and their binding regions to nuclear receptors and other co-activators (e.g., p300 and SRC1) are apparently different. While the binding region for nuclear receptors and co-activators in ASC1 (consisting of 581 amino acids) is restricted to the single zinc finger domain, their binding regions are located in different domains scattered throughout in ASC2 (2,063 amino acids). Furthermore, ASC2 is not modified by UFM1 even under conditions that UFM1-conjugating machinery was overexpressed (data not shown). Neither p300 nor SRC1 could be ufmylated. Thus, it appears that ASC2 employs itself as the platform that recruits the necessary components for promotion of nuclear receptor transactivation, while ASC1 primarily uses poly-UFM1 chains.

Induction of ASC1 ufmylation was not limited to E_2, but could also occur in the presence of other ligands if their cognate nuclear receptors are present in cells. For example, DHT, which is an agonist of androgen receptor (AR), effectively induced ASC1 ufmylation in LNCaP cells, but not in AR-negative cells, such as PC3 cells.

Thus, it appears likely that poly-UFM1 chains conjugated to ASC1 serves as a common scaffold at least for steroid hormone nuclear receptors. I are currently investigating the effect of ASC1 ufmylation on transactivation of AR, and its role in development of prostate cancer.

Breast cancer is one of the most prevailing forms of woman cancers. It has been well documented that E_2 plays critical roles in the pathogenesis and development of breast cancer (Castoria et al., 2010; Umar et al., 2012). Therefore, patients with ERα-positive tumors have been treated with tamoxifen, which blocks the binding of E_2 to ERα, or with aromatase inhibitors, which prevents the synthesis of E_2 (Beelen et al., 2012; Jordan, 2007; Nilsson et al., 2011; Renoir, 2012). While these treatments are effective, many patients inevitably develop the drug-resistant invasive tumors. In this study, I showed that E_2-mediated ASC1 ufmylation is required for ERα transactivation and tumor formation in vivo. Furthermore, UFM1-conjugating machinery was found to be dramatically up-regulated in ERα-positive tumor tissues, but not in ERα-negative tissues, implicating its ERα-specific oncogenic function. Therefore, UBA5

and other components of UFM1-conjugating machinery involved in ASC1 ufmylation could be used as targets for development of new therapeutic drugs against ERα-positive breast cancer. Of also importance was the finding that UfSP2 knockdown leads to a dramatic increase in cell proliferation, anchorage-independent colony formation, and tumor formation in vivo, implicating its potential role as a tumor suppressor. So far, little information on the incidence of mutations in the UfSP2 gene is available in the database for breast cancer patients, perhaps because the biological function of UfSP2 has been illusive before this study. Therefore, the search for mutations in the UfSP2 gene would potentially be important for diagnosis of ERα-positive breast cancers.

REFERENCE

Azfer, A., Niu, J., Rogers, L.M., Adamski, F.M., and Kolattukudy, P.E. (2006) Activation of endoplasmic reticulum stress response during the development of ischemic heart disease. Am. J. Physiol. Heart Circ. Physiol. 291, H1411-1420.

Beelen, K., Zwart, W., and Linn, S.C. (2012) Can predictive biomarkers in breast cancer guide adjuvant endocrine therapy? Nat. Rev. Clin. Oncol. 9, 529-541.

Caira, F., Antonson, P., Pelto-Huikko, M., Treuter, E., and Gustafsson, J.A. (2000) Cloning and characterization of RAP250, a novel nuclear receptor coactivator. J. Biol. Chem. 275, 5308-5317.

Castoria, G., Migliaccio, A., Giovannelli, P., and Auricchio, F. (2010) Cell proliferation regulated by estradiol receptor: Therapeutic implications. Steroids 75, 524-527.

Shanle EK, Xu W. (2010) Selectively targeting estrogen receptors for cancer treatment. Adv. Drug Deliv. Rev. 62, 1265-76.

Gannavaram, S., Sharma, P., Duncan, R.C., Salotra, P., and Nakhasi, H.L. (2011) Mitochondrial associated ubiquitin fold modifier-1 mediated protein conjugation in Leishmania donovani. PLoS One 6, e16156.

Gougelet A, Bouclier C, Marsaud V, Maillard S, Mueller SO, Korach KS, Renoir JM (2005) Estrogen receptor α and β subtype expression and transactivation capacity are differentially affected by receptor-, hsp90- and immunophilin-ligands in human breast cancer cells. J. Steroid Biochem. Mol. Biol. 94, 71–81

Green, K.A., and Carroll, J.S. (2007) Oestrogen-receptor-mediated transcription and the influence of co-factors and chromatin state. Nat. Rev. Cancer 7, 713-722.

Ha, B.H., Ahn, H.C., Kang, S.H., Tanaka, K., Chung, C.H., and Kim, E.E. (2008) Structural basis for Ufm1 processing by UfSP1. J. Biol. Chem. 283, 14893-14900.

Ha, B.H., Jeon, Y.J., Shin, S.C., Tatsumi, K., Komatsu, M., Tanaka, K., Watson, C.M., Wallis, G., Chung, C.H., and Kim, E.E. (2011) Structure of ubiquitin-fold modifier 1-specific protease UfSP2. J. Biol. Chem. 286, 10248-10257.

Hanstein, B., Eckner, R., DiRenzo, J., Halachmi, S., Liu, H., Searcy, B., Kurokawa, R.,

and Brown, M. (1996) p300 is a component of an estrogen receptor coactivator complex. Proc. Natl. Acad. Sci. USA 93, 11540-11545.

Hassig, C.A., and Schreiber, S.L. (1997) Nuclear histone acetylases and deacetylases and transcriptional regulation: HATs off to HDACs. Curr. Opin. Chem. Biol. 1, 300-308.

Hermanson, O., Glass, C.K., and Rosenfeld, M.G. (2002) Nuclear receptor coregulators: multiple modes of modification. Trends Endocrinol. Metab. 13, 55-60.

Hoeller, D., Hecker, C.M., and Dikic, I. (2006) Ubiquitin and ubiquitin-like proteins in cancer pathogenesis. Nat. Rev. Cancer 6, 776-788.

Jeon, Y.J., Jo, M.G., Yoo, H.M., Hong, S.H., Park, J.M., Ka, S.H., Oh, K.H., Seol, J.H., Jung, Y.K., and Chung, C.H. (2012) Chemosensitivity is controlled by p63 modification with ubiquitin-like protein ISG15. J. Clin. Invest. 122, 2622-2636.

Jeon, Y.J., Yoo, H.M., and Chung, C.H. (2010) ISG15 and immune diseases. Biochim. Biophys. Acta 1802, 485-496.

Jordan, V.C. (2007) Chemoprevention of breast cancer with selective oestrogen-receptor modulators. Nat. Rev. Cancer 7, 46-53.

Jozwik, K.M., and Carroll, J.S. (2012) Pioneer factors in hormone-dependent cancers. Nat. Rev. Cancer 12, 381-385.

Kang, S.H., Kim, G.R., Seong, M., Baek, S.H., Seol, J.H., Bang, O.S., Ovaa, H., Tatsumi, K., Komatsu, M., Tanaka, K., et al. (2007) Two novel ubiquitin-fold modifier 1 (Ufm1)-specific proteases, UfSP1 and UfSP2. J. Biol. Chem. 282, 5256-5262.

Kim, H.J., Yi, J.Y., Sung, H.S., Moore, D.D., Jhun, B.H., Lee, Y.C., and Lee, J.W. (1999) Activating signal cointegrator 1, a novel transcription coactivator of nuclear receptors, and its cytosolic localization under conditions of serum deprivation. Mol. Cell. Biol. 19, 6323-6332.

Klinge, C.M. (2001) Estrogen receptor interaction with estrogen response elements. Nucleic Acids Res. 29, 2905-2919.

Ko, L., Cardona, G.R., and Chin, W.W. (2000) Thyroid hormone receptor-binding

protein, an LXXLL motif-containing protein, functions as a general coactivator. Proc. Natl. Acad. Sci. USA 97, 6212-6217.

Kobayashi Y, Kitamoto T, Masuhiro Y, Watanabe M, Kase T, Metzger D, Yanagisawa J, Kato S. (2000) p300 mediates functional synergism between AF-1 and AF-2 of estrogen receptor α and β by interacting directly with the N-terminal A/B domains. J. Biol. Chem. 275, 15645–15651.

Komatsu, M., Chiba, T., Tatsumi, K., Iemura, S., Tanida, I., Okazaki, N., Ueno, T., Kominami, E., Natsume, T., and Tanaka, K. (2004) A novel protein-conjugating system for Ufm1, a ubiquitin-fold modifier. EMBO J. 23, 1977-1986.

Kulathu, Y., and Komander, D. (2012) Atypical ubiquitylation - the unexplored world of polyubiquitin beyond Lys48 and Lys63 linkages. Nat. Rev. Mol. Cell Biol. 13, 508-523.

Kwon, J., Cho, H.J., Han, S.H., No, J.G., Kwon, J.Y., and Kim, H. (2010) A novel LZAP-binding protein, NLBP, inhibits cell invasion. J. Biol. Chem. 285, 12232-12240.

Lee, D.Y., Teyssier, C., Strahl, B.D., and Stallcup, M.R. (2005) Role of protein methylation in regulation of transcription. Endocr. Rev. 26, 147-170.

Lee, J.W., Choi, H.S., Gyuris, J., Brent, R., and Moore, D.D. (1995) Two classes of proteins dependent on either the presence or absence of thyroid hormone for interaction with the thyroid hormone receptor. Mol. Endocrinol. 9, 243-254.

Lee, S.K., Anzick, S.L., Choi, J.E., Bubendorf, L., Guan, X.Y., Jung, Y.K., Kallioniemi, O.P., Kononen, J., Trent, J.M., Azorsa, D., et al. (1999) A nuclear factor, ASC-2, as a cancer-amplified transcriptional coactivator essential for ligand-dependent transactivation by nuclear receptors in vivo. J. Biol. Chem. 274, 34283-34293.

Le Romancer M, Poulard C, Cohen P, Sentis S, Renoir JM, Corbo L. (2011) Cracking the estrogen receptor's posttranslational code in breast tumors. Endocr Rev. 32, 597-622

Lemaire, K., Moura, R.F., Granvik, M., Igoillo-Esteve, M., Hohmeier, H.E., Hendrickx, N., Newgard, C.B., Waelkens, E., Cnop, M., and Schuit, F. (2011)

Ubiquitin fold modifier 1 (UFM1) and its target UFBP1 protect pancreatic beta cells from ER stress-induced apoptosis. PLoS One 6, e18517.

Liang, J., and Shang, Y. (2013) Estrogen and cancer. Annu. Rev. Physiol. 75, 225-240.

Lonard, D.M., and O'Malley, B.W. (2006) The expanding cosmos of nuclear receptor coactivators. Cell 125:411–414

Lonard, D.M., and O'Malley B, W. (2007) Nuclear receptor coregulators: judges, juries, and executioners of cellular regulation. Mol. Cell 27, 691-700.

Mahajan, M.A., and Samuels, H.H. (2000) A new family of nuclear receptor coregulators that integrate nuclear receptor signaling through CREB-binding protein. Mol. Cell. Biol. 20, 5048-5063.

Mahajan, M.A., and Samuels, H.H. (2005) Nuclear hormone receptor coregulator: role in hormone action, metabolism, growth, and development. Endocr. Rev. 26, 583-597.

Mahajan, M.A., and Samuels, H.H. (2008) Nuclear receptor coactivator/coregulator NCoA6(NRC) is a pleiotropic coregulator involved in transcription, cell survival,

growth and development. Nucl. Recept. Signal. 6, e002.

Mizushima, T., Tatsumi, K., Ozaki, Y., Kawakami, T., Suzuki, A., Ogasahara, K., Komatsu, M., Kominami, E., Tanaka, K., and Yamane, T. (2007) Crystal structure of Ufc1, the Ufm1-conjugating enzyme. Biochem. Biophys. Res. Commun. 362, 1079-1084.

Neziri, D., Ilhan, A., Maj, M., Majdic, O., Baumgartner-Parzer, S., Cohen, G., Base, W., and Wagner, L. (2010) Cloning and molecular characterization of Dashurin encoded by C20orf116, a PCI-domain containing protein. Biochim. Biophys. Acta 1800, 430-438.

Nilsson, S., Koehler, K.F., and Gustafsson, J.A. (2011) Development of subtype-selective oestrogen receptor-based therapeutics. Nat. Rev. Drug Discov. 10, 778-792.

Nilsson, S., Makela, S., Treuter, E., Tujague, M., Thomsen, J., Andersson, G., Enmark, E., Pettersson, K., Warner, M., and Gustafsson, J.A. (2001) Mechanisms of estrogen action. Physiol. Rev. 81, 1535-1565.

Osborne, C.K., and Schiff, R. (2011) Mechanisms of endocrine resistance in breast cancer. Annu. Rev. Med. 62, 233-247.

Perissi, V., Jepsen, K., Glass, C.K., and Rosenfeld MG (2010) Deconstructing repression: evolving models of co-repressor action. Nat Rev Genet 11:109–123

Renoir, J.M. (2012) Estradiol receptors in breast cancer cells: associated co-factors as targets for new therapeutic approaches. Steroids 77, 1249-1261.

Robyr, D., Wolffe, A.P., and Wahli, W. (2000) Nuclear hormone receptor coregulators in action: diversity for shared tasks. Mol. Endocrinol. 14:329–347

Sasakawa, H., Sakata, E., Yamaguchi, Y., Komatsu, M., Tatsumi, K., Kominami, E., Tanaka, K., and Kato, K. (2006) Solution structure and dynamics of Ufm1, a ubiquitin-fold modifier 1. Biochem. Biophys. Res. Commun. 343, 21-26.

Schmidt, D., and Muller, S. (2003) PIAS/SUMO: new partners in transcriptional regulation. Cell. Mol. Life Sci. 60, 2561-2574.

Schulman, B.A., and Harper, J.W. (2009) Ubiquitin-like protein activation by E1 enzymes: the apex for downstream signalling pathways. Nat. Rev. Mol. Cell Biol.

10, 319-331.

Shao, W., Keeton, E.K., McDonnell, D.P., and Brown, M. (2004) Coactivator AIB1 links estrogen receptor transcriptional activity and stability. Proc. Natl. Acad. Sci. USA 101, 11599-11604.

Skrzypczak, M., Kapka-Skrzypczak, L., Cyranka, M., Treeck, O., Wrobel, A., and Matosiuk, D. (2013) Nuclear estrogen receptors co-activation mechanisms. Curr. Med. Chem. 20, 3317-38.

Smith, C.L., Onate, S.A., Tsai, M.J., and O'Malley, B.W. (1996) CREB binding protein acts synergistically with steroid receptor coactivator-1 to enhance steroid receptor-dependent transcription. Proc. Natl. Acad. Sci. USA 93, 8884-8888.

Tatsumi, K., Sou, Y.S., Tada, N., Nakamura, E., Iemura, S., Natsume, T., Kang, S.H., Chung, C.H., Kasahara, M., Kominami, E., Komatsu, M., and Tanaka, K. (2010) A novel type of E3 ligase for the Ufm1 conjugation system. J. Biol. Chem. 285, 5417-5427.

Tatsumi, K., Yamamoto-Mukai, H., Shimizu, R., Waguri, S., Sou, Y.S., Sakamoto, A.,

Taya, C., Shitara, H., Hara, T., Chung, C.H., Komatsu, M., and Tanaka, K. (2011) The Ufm1-activating enzyme Uba5 is indispensable for erythroid differentiation in mice. Nat. Commun. 2, 181.

Umar, A., Dunn, B.K., and Greenwald, P. (2012) Future directions in cancer prevention. Nat. Rev. Cancer 12, 835-848.

Wu, H., Sun, L., Zhang, Y., Chen, Y., Shi, B., Li, R., Wang, Y., Liang, J., Fan, D., Wu, G., et al. (2006) Coordinated regulation of AIB1 transcriptional activity by sumoylation and phosphorylation. J. Biol. Chem. 281, 21848-21856.

Wu, J., Lei, G., Mei, M., Tang, Y., and Li, H. (2010) A novel C53/LZAP-interacting protein regulates stability of C53/LZAP and DDRGK domain-containing Protein 1 (DDRGK1) and modulates NF-kappaB signaling. J. Biol. Chem. 285, 15126-15136.

Xu, J., Wu, R.C., and O'Malley, B.W. (2009) Normal and cancer-related functions of the p160 steroid receptor co-activator (SRC) family. Nat. Rev. Cancer 9, 615-630.

Zhang, Y., Zhang, M., Wu, J., Lei, G., and Li, H. (2012) Transcriptional regulation of

the Ufm1 conjugation system in response to disturbance of the endoplasmic reticulum homeostasis and inhibition of vesicle trafficking. PLoS One 7, e48587.

Zheng, M., Gu, X., Zheng, D., Yang, Z., Li, F., Zhao, J., Xie, Y., Ji, C., and Mao, Y. (2008) UBE1DC1, an ubiquitin-activating enzyme, activates two different ubiquitin-like proteins. J. Cell. Biochem. 104, 2324-2334.

국문 초록

유비퀴틴-접합 변형체 1(UFM1)은 최근에 발견된 유비퀴틴-유사 단백질(Ubl)로, 그 3차 구조가 유비퀴틴(Ub)과 유사성이 매우 높다. UFM1은 유비퀴틴 및 다른 유사단백질들과 같이 카르복시 말단에 있는 glycine을 통해 타겟 단백질에 결합되며, UFM1 활성효소인 UBA5, UFM1 접합효소인 UFC1, UFM1 결합효소인 UFL1의 순차적 반응을 통해 결합된다. UFM1 결합은 가역반응으로 두개의 UFM1-특이적 단백질 분해효소들인 UfSP1, UfSP2에 의해 타겟 단백질로부터 유리된다. UfSP들은 또한 UFM1 전구체를 성숙된 상태로 만드는데도 관여한다. UFM1 결합 및 유리 시스템은 *C.elegans* 부터 인간에까지 잘 보존되어 있으며(하지만 yeast나 원핵생물에는 보존되어있지 않음) 이는 이 시스템이 다세포 생물에서 중요한 역할을 함을 시사한다. 그러나 UFM1에 의해 변형되는 타겟 단백질이나 결합 시스템의 기능에 대해서는 아직 알려진 바가 많지 않다.

질량분석기를 이용하여 activating signal cointegrator 1 (ASC1: thyroid hormone receptor interactor 4, TRIP4 로도 불려짐)을 UFM1과 결합하는 후보 타겟 단백질로 찾을 수 있었다. ASC1은 RAR 알파, 스테로이드 수용체, NF-κB 등 다양한 전사 인자의 보조 활성자로서 기능한다. 또한 다른 전사 보조활성인자로 알려진 p300이나 SRC1등과 복합체를 형성하며 핵 수용체들의 전사 활성을 촉진시킨다.

과 발현 조건 하에서 ASC1은 ATP 의존적으로 UFM1 시스템 (즉, UFM1, UBA5, UFC1 및 UFL1)에 의해 poly-ufmylation되고 이러한 변형은 기존에 ufmylation 타겟 단백질로 이미 알려진 C20orf116에 의하여 극적으로 증대될 수 있다. 이런 증대효과는 C20orf116자체의 ufmylation을 필요로 하며 이는 C20orf116이 타겟 단밸질로서 작용할 뿐만 아니라 UFM1 시스템의 한 구성요소로 작용함을 제시한다. C20orf116 도 UFM1과 결합 할 수 있는 능력에 따라 UFBP1이라고 명명된 바 있으며 C20orf116를 UFBP1으로 지칭 할 수 있다.

ASC1은 실제로 UFM1과 결합하며 이 변형(ufmylation)이 인간

유방암 발달에 매우 중요함을 밝혔다. 17-베타 에스트라디올 리간드가 없을 때에는 UFM1 특이적 분해 효소인 UfSP2에 의해 ASC1이 de-ufmylation 된다. 그러나 리간드가 존재할 때에는 에스트로겐 수용체 알파(ERα)가 UfSP2를 대체하면서 ASC1의 de-ufmylation을 방지한다.

ASC1에 poly-UFM1 사슬이 결합되면 이는 에스트로겐 수용체 알파의 타겟 유전자들의 전사활성 촉진을 위해 프로모터 부위로 p300과 SRC1 단백질을 모아주는 scaffold로 작용한다. ASC1을 과발현 시키거나 UfSP2를 knockdown 시키면 생쥐 생체 내에서 암 형성이 촉진된다. 반면에 ASC1의 UFM1결합이 결여된 돌연변이를 과발현 시키거나, UFM1의 활성효소인 UBA5를 knockdown시키면 암 형성이 방지된다. 더욱이 에스트로겐 수용체 알파가 존재하는 유방암에서 UBA5 효소를 포함한 UFM1 결합 machinery들이 높은 레벨로 조절되고 있다. 이러한 발견들은 ASC1의 UFM1결합이 에스트로겐 수용체 알파의 전사활성을 촉진시켜 유방암의 발달에 있어서 중요한 역할을 함을 제시한다.

주요어: Ubiquitin-fold modifier 1 (UFM1), UFM1-specific protease (UfSP2), Activating signal cointegrator 1 (ASC1), 17b-에스트라디올, ERα, 유방암

학번 : 2009-30084